Energy Conversion and Management 171 (2018) 1843–1859

Contents lists available at ScienceDirect

Energy Conversion and Management

journal homepage: www.elsevier.com/locate/enconman

Parameter estimation of solar cells diode models by an improved opposition-based whale optimization algorithm

Mohamed Abd Elaziz[a,1], Diego Oliva[b,*,1]

[a] Department of Mathematics, Faculty of Science, Zagazig, University, Zagazig, Egypt
[b] Departamento de Computación, Universidad de Guadalajara, CUCEI, Av. Revolución 1500, Guadalajara, Jal, Mexico

ARTICLE INFO

Keywords:
Photo voltaic cells
Whale optimization
Opposition-based learning
Solar cell modeling

ABSTRACT

Solar cells are considered as a clean source of energy, and their application includes industrial and domestic users. Most of the algorithms used to design solar cells are tested (and used) only for domestic implementations. However, it is necessary to have accurate mechanisms for solar cell design that can be used in both industrial and domestic energy systems. To achieve this goal, this article introduces an improved version of the whale optimization Algorithm that uses the opposition-based learning to enhance the exploration of the search space. This algorithm is applied to estimate the parameters of solar cells using three different diode models. Such models are the single diode model, the double diode model and the three diode model, each of them has different internal parameters that must be accurately estimated in order to have a good performance of the solar cells. The inclusion of the three diode model is due it represents a more accurate representation of the solar cells behavior in industrial applications. For experiments and comparisons, there are used similar approaches and datasets from solar cells and photovoltaic modules. Moreover, the proposed method has also been tested over different benchmark optimization functions to verify its exploration capabilities. The experiments and comparisons support the performance of the proposed approach in complex optimization problems.

1. Introduction

Nowadays Solar Energy (SE) is extensively explored and rapidly growing because the solar radiation is present in all parts of the world [1]. The use of SE not only helps to electricity production but also it reduces the pollution since it is not necessary to burn any fuel to produce energy [1]. In this sense, the research in SE has also increased from 1996 to 2016 [2], through these years several publications and projects have been developed in this field. This is the evidence of the necessity of proposing new methodologies for the problems presents in this area. In this context, the use of Photovoltaic modules (PV) composed of Solar Cells (SC) has also been increased. According to [3] in 2016 the prices of PV systems were considerably reduced and the demand for PV devices growth in different developing countries. One of the main drawbacks of PV modules is their efficiency that is affected by uncontrolled variables like weather [4]. Moreover, their the maintenance is expensive [5]. Considering the points previously mentioned they are required new methods for the design of PV modules an SC.

The process of design SC consists in the estimation of the parameters using a mathematical model. Such model simulates the variables that control the behavior of a real SC, and the aim is to represent the relationship between the current vs. voltage (I-V). They are two models that are commonly used for this task, the Single Diode (SD) model and the Double Diode (DD). The SD and DD models are electronic circuits that can describe the nonlinearities of the SC. Basically, in the SD and DD, they are included photo-generated current, the diode saturation current, the series resistance, and the diode ideality factor. An exact configuration of such elements is reflected in the performance of the SC or PV modules. In the case of the SD, they are used five parameters to describe the SC. Meanwhile, the DD employs seven. These parameters should be adequately estimated to generate a right balance between I and V. These diode models are used in several related studies, and they provide satisfactory results. However, SD and DD circuits are defined for domestic solar cells, and their performance has been only tested for this kind of problems. To overcome this situation, it is introduced a Three Diode (TD) model for solar cells that can also be used for photovoltaic modules [6]. The TD has nine parameters that are used to simulate the behavior of the PV modules. The use of such parameters increases the accuracy of the output and permits to generate a model for industrial applications.

* Corresponding author.
E-mail addresses: abd_el_aziz_m@yahoo.com (M. Abd Elaziz), diego.oliva@cucei.udg.mx (D. Oliva).
[1] International Research Team.

https://doi.org/10.1016/j.enconman.2018.05.062
Received 19 September 2017; Received in revised form 7 May 2018; Accepted 17 May 2018
Available online 10 July 2018
0196-8904/

Nomenclature

WOA	Whale Optimization Algorithm
OBL	Opposition-Based Learning
NVTR	total numbers that the algorithm reached to value-to-reach
STD	Standard Deviation
Mean	Mean of fitness values
R_{err}	Relative Error
NR_{err}	Normalized Relative Error
MAE	Mean Absolute Error
NMAE	Normalized MAE
SE	Solar Energy
NRMSE	Normalized RMSE
MBE	Mean Bias Error
NMBE	Normalize MBE
N_E	number of experimental data$N_E = 26$
$\min(I_{te})$	minimum values ofI_{te}
$\max(I_{te})$	maximum values ofI_{te}
G	irradiance
N_r	total number of runs
SD	single diode model
DD	double diode model
R_s	series resistances
R_{sh}	shunt resistances
n_1, n_2, n_3	non-physical ideality factors
q	magnitude of charge on an electron
k	Boltzmann constant
T°	cell temperature (°K)
RMSE	root mean square error
x_{best}	the best position (solution)
$x(t)$	the current position of whale (solution)
D	distance between two solutions
t	current iteration
C and A	coefficient vectors for WOA
$\overline{x}$	opposite solution
N	population size
SR	Success Rate
I_{sd}, I_{sd2}, I_{sd3}	diode saturation currents
I_{sh}	shunt resistor current
V_t	terminal voltage
TD	three diode model
I_{ph}	photogenerated current source

One of the main drawbacks of using diode circuits is that is necessary to configure a set of parameters in order to obtain the desired output. This problem could be addressed from an optimization point of view. In the related literature, they exist some implementation that uses numerical methods to search for the optimal parameter configuration. For example in [7], it is introduced a nonlinear least-squares algorithm that considers the Newton model for the extraction of SC parameters. Another interesting method was proposed in [8], it presents a Lambert W-function based representation for the estimation of the parameters of the DD model. Other alternatives include the use of a co-content function to generate analytical solution of the I-V characteristics [9]. In the same context, in [10] they have been compared three analytical methods for extract SC parameters using the SD model, in this study it is verified that curve fitting approach provide more inconsistencies in the results. Tabular methods have also been applied in PV systems [11], providing good results but using a considerable amount of computational resources. There exist some interesting studies and surveys that analyze different methods, for example in [12] is provided a comparison between Newton-Raphson method, the Levenberg–Marquardt algorithm. Meanwhile, in [13] are evaluated six different techniques based on mathematical functions. The use of the deterministic techniques (as the previously mentioned) implies several restrictions such as differentiability and convexity to be correctly applied [12]. Therefore, their outputs are affected by the initial solutions, which lead to local optima. For example, the application of the Newton-Rapson method [14] to the DD model, which presents a significant deviation among the real, and the estimated of the current and voltage values [15]. Other drawbacks of these approaches are that they are computationally expensive, and they are only applied for SD or DD.

On the other hand, the use of Evolutionary Computation Algorithms (ECA) to estimate the parameter of PV modules and SC has been extended in last years. ECA are able to explore multimodal search spaces using different operators to find the best solution. To affront the estimation of parameters of SC as an optimization problem the Root Mean Squared Error (RMSE) is used as an objective function. The RMSE measures the difference that exists between a set of experimental data (or information provided by the manufacturer) and the estimated output of the diode model.

One of the main advantages of ECA applied to PV modules is that they do not require a priori information about the search space. In this context, several approaches are proposed in the related literature. For example, in [16] the Genetic Algorithms (GA) are used to increase the accuracy of the parameters estimated of the DD. The Particle Swarm Optimization (PSO) has also been used to estimate the parameters of solar cells using SD and DD models [17], for the experiments of this study the authors employ both synthetic and experimental information. Another interesting approach uses the Simulated Annealing (SA) to compute the values of the SD and DD [18], according with the authors the results provided by SA are better than other approaches used for comparisons. In 2016 it was proposed the use of a relative new method called the Cat Swarm Optimization (CSO) for finding the best parameter of SC using the SD and the DD [19]. Moreover in [19] the CSO has also been compared with different methods to verify the quality of the solutions. In [20] the Bacterial Foraging Algorithm (BFA) is introduced as an alternative to accurately models the characteristics of a SC using a new equation proposed by the authors. In the same context, in [21] they have been proposed different versions of the Harmony Search (HS) algorithm to identify the unknown parameters of the solar cell single and double diode models. Meanwhile the Simplified Teaching-Learning Based Optimization (STBLO) is introduced in [22] for the identification of solar cell models, this approach is an improved version of the Teaching-Learning Based Optimization (TBLO). Such methods provide good results but to increase the accuracy of the results they have also been introduced some modifications of standard ECA. The chaotic maps are commonly used instead random numbers in the iterative process of ECA's. The implementation of such maps has also been extended for solar cells, for example the Chaotic PSO [17] is a version that provides better results that the classic PSO for SD and DD model. In the same context, the Chaotic Whale Optimization Algorithm (CWOA) [23], uses the chaotic maps to generate more accurate solutions for SD and DD using information from real SC and photovoltaic modules. In [24] it is introduced the Chaotic Improved Artificial Bee Colony (CIABC), this method includes the use of chaotic maps and also a modification that perseveres the information from previous iterations. The CIABC provide more accurate results even with the presence of noise in the dataset. Meanwhile, in the Chaotic Gravitational Search Algorithm (CGSA) [25] is an improved version that used the chaos to compute an internal parameter in the optimization process. The CGSA is applied in [25] to solve the problem of accurate PV cell parameter estimation. Such methods are efficient, but they still have problems with accuracy. In real-life problems like PV or SC is desired to have accurate outputs to reduce the cost of the energy systems [26]. Additionally, only the PSO has been used for TD model [6], and all the other approaches consider only SD or DD.

In the related literature there exist several ECA, for example, the Whale Optimization Algorithm (WOA) that was proposed in 2016 for global optimization problems [27]. The WOA is inspired by the hunting behavior of the humpback whales. In WOA each solution is considered as a whale that takes a new position in the search space considering as a reference the best element of the group. WOA has different parameters to control the behavior of the population, and its main advantage is the simulation of the mechanism to chase the prey. To imitate this process, it is considered the randomness of the best search agents and the spiral movement hat helps to mimic the bubble-net attraction process of humpback whales [27]. Such behaviour is the main difference that WOA has with other ECA. In this way, WOA has only few parameters to be tuned, and they are adjusted along to the iterations. However, one of the main drawbacks of WOA is that a random variable controls the adaptive parameters. Another problem of WOA is the premature convergence; it happens mainly in problems that possess high multimodal search spaces. The performance of WOA is supported by experiments over different benchmark functions and engineering design benchmark problems [27]. Moreover, WOA has also been applied of liver segmentation using medical images [28]. Another interesting implementation is for optimal sizing of renewable resources for loss reduction in distribution systems [29]. However, such approaches consider the standard version of WOA. To overcome the problems of WOA they have been proposed some modified versions, for example, the use of chaotic distributions for set the control parameters [23] or the hybridization of WOA with Lévy flights [30].

In order to avoid the exploration problems of ECA in 2005 Tizhoosh proposes the Opposition-Based Learning (OBL) [31]. The OBL is used to generate the opposite position of a candidate solution; this process permits to explore the search space in two senses at the same time. Considering the objective function values, the OBL selects the best elements from a set comforted by the candidate and the opposite solutions. The OBL rule can be used in the initialization process or in any part of the ECA where a solution is modified. Different ECA's have been amended using OBL providing better results than the standard versions; some improvements are for example the Opposition Based Electromagnetism-Like (OBEMO) [32], where OBL helps to increase the speed of convergence of EMO. Meanwhile, in [33], the OBL is used for multiobjective optimization problems. The combination of OBL has also been extended for engineering implementations; in [34] the OBL is used to find the optimal parameter values in control engineering in combination with the Shuffled Frog Leaping (SFL) algorithm. Meanwhile, the problem of economic load dispatch has been addressed by the OB Krill Herd (KH) algorithm in [35]. In the same context, the OB Sine Cosine Algorithm (OBSCA) has been recently introduced as an alternative approach for engineering problems [36].

This paper presents an improved version of Whale Optimization Algorithm using OBL (called OBWOA) for parameter estimation of solar cells and photovoltaic modules. OBL is used to compute the opposite position of the whales' population; this process occurs in the initialization and during the evolution of the candidate solutions. The OBWOA has also been tested over a set of benchmark functions, providing evidence of its capabilities to find the best solutions in complex search spaces. Moreover, in the application of OBWOA for SC and PV modules, they are considered the SD, DD, and TD. In this sense, the OBWOA also prove that can be used in real optimization problems with different dimensions. Summarizing, the goals of this paper are (1) the modification of WOA using OBL for global optimization problems and (2) the implementation of the proposed OBWOA for the estimate the parameters of SC diode models.

The remainder paper is organized as follows: Section 2 defines the diode models for SC and how the problem can be addressed by optimization algorithms. In Section 3 are introduced the concepts of WOA and OBL. Section 4 explains the proposed OBWOA for SC. Section 5 presents the experiments using the set of benchmark functions and the data for SC. Finally, in Section 6 are provided the conclusions.

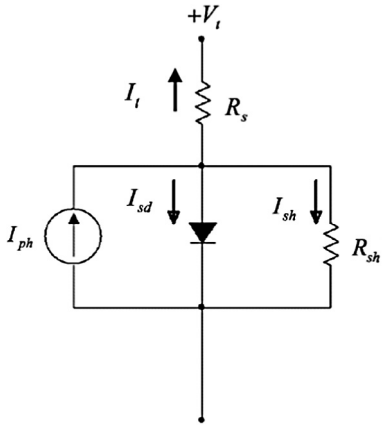

Fig. 1. Equivalent circuit of the dingle diode model of a SC.

2. Solar cells diode circuit models

For the design of solar cells and PV modules, it is required a mathematical model to estimate the internal parameters of SC analytically. In this context, the behavior of the SC is modeled using electronic circuits based on diodes. The Single Diode (SD) and the Double Diode (DD) models are extensively utilized in the related literature for SC and PV modules [37]. Moreover, in recent years it has been proposed the use of a Three Diode (TD) circuit for the same aim [6]. This section presents the concepts of the three models and how they can adapt as an optimization problem.

2.1. Single diode model

This model has only one diode that is responsible for shunting the photogenerated current sourceI_{ph}. The diode works as a rectifier in the circuit, here it is also considered the non-physical ideality of the diode using an extra parameter [18]. The simplicity of this model makes easy to apply. The problem with the SD model is to estimate five parameters because an optimal configuration is reflected on the output of the model. Fig. 1 shows the circuit for the SD model.

In Fig. 1, the SC current (I_t) is computed as in the following equation:

$$I_t = I_{ph} - I_{sd} - I_{sh} \tag{1}$$

where I_t, I_{ph}, I_{sd} and I_{sh} represent the terminal, the photogenerated, the diode and the shunt resistor current, respectively. Considering the equivalent Shockley diode equation is possible to manipulate the internal parameters of the diode to generate a more accurate output. Thus Eq. (1) can be rewritten as:

$$I_t = I_{ph} - I_{sd}\left[\exp\left(\frac{q(V_t + R_s \cdot I_t)}{n \cdot k \cdot T}\right) - 1\right] - \frac{V_t + R_s \cdot I_t}{R_{sh}} \tag{2}$$

where V_t represents the terminal voltage, I_{sd} is defined as the diode saturation currents, R_s and R_{sh} represent the series and the shunt resistances, respectively. Meanwhile, the non-physical ideality factor is the variable *n*. Since in Eq. (2) is embedded the Shockley diode equation, some physical constants are also included. The magnitude of charge on an electron $q = 1.602 \times 10^{-19}$ C (coulombs), the Boltzmann constant $k = 1.380 \times 10^{-23}$ (J/K) and T that is the cell temperature (K). As was previosly mentioned, a proper configuration of this model is reflected in the output provided by V_t and I_t. To successfully reach this goal, the problem can be summarized to estimate the values of accurately.

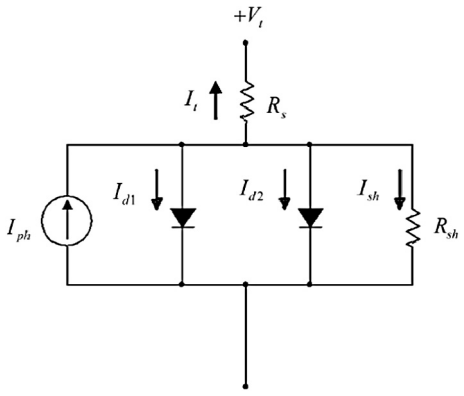

Fig. 2. Equivalent circuit of the double diode model of a SC.

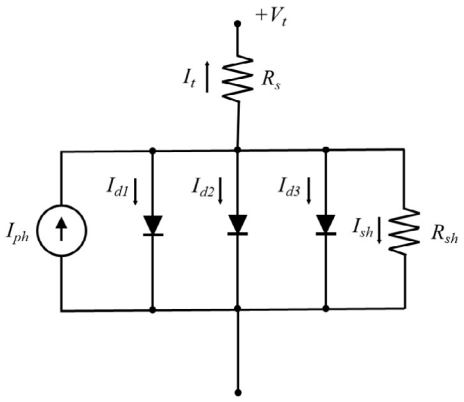

Fig. 3. Equivalent circuit of the three diode model of an SC.

2.2. Double diode model

The SD is a good approach to the real SC, but according to the related literature, it is not entirely accurate for different implementation [21]. For that reason it is proposed de Double Diode (DD) model, it considers one diode as a rectifier and the second diode is used to design the recombination current and other non-idealities of the SC [21]. Fig. 2 shows the DD circuit in which to shunt the photogenerated current source are used the two diodes.

Considering Fig. 2 Eq. (1) can be rewritten as follows:

$$I_t = I_{ph} - I_{d1} - I_{d2} - I_{sh} \tag{3}$$

From Eq. (3) the I_{d1} and I_{d2} represents the currents of the first and second diode, respectively. The rest of the elements are the same to Eq. (1). To modify the internal configuration of the diodes, the Shockley equivalence is used, and Eq. (3) is then modified as in Eq. (4).

$$I_t = I_{ph} - I_{sd1}\left[\exp\left(\frac{q(V_t + R_s \cdot I_t)}{n_1 \cdot k \cdot T}\right) - 1\right] - I_{sd2}\left[\exp\left(\frac{q(V_t + R_s \cdot I_t)}{n_2 \cdot k \cdot T}\right) - 1\right] \ldots - \frac{V_t + R_s \cdot I_t}{R_{sh}} \tag{4}$$

Similar to SD in DD the I_{sd1} and I_{sd1} are the diffusion and saturation current, represented for each diode (*d1* and *d1*). The diffusion and recombination diode ideality factors are defined by n_1 and n_2. The remaining elements are previously defined in the description of Eq. (2). Considering that the DD circuit has seven undefined parameters that should be accurately estimated, such elements are R_s, R_{sh}, I_{ph}, I_{sd1}, I_{sd2}, n_1 and n_2.

2.3. Three diode model

The use of efficient SC and PV modules is desired in energy systems, in this sense in is necessary to use accurate models of these devices. The Three Diode (TD) model is then defined as an alternative to SD and DD; the main advantage is that it can be used for industrial applications [6]. In the TD circuit (presented in Fig. 3) the two diodes are similar to DD model, and the inclusion of a third diode in parallel is to consider the contribution of it based on the recombination in the defect regions. According to [38], the three diodes must be designed considering a proper configuration of their internal parameters.

With the incorporation of the third diode, Eq. (1) is redefined as:

$$I_t = I_{ph} - I_{d1} - I_{d2} - I_{d3} - I_{sh} \tag{5}$$

The TD is an extension of SD and DD, in this way as was previously mentioned the third diode models the defects that occur in the recombination. Using the Shockley equivalence, Eq. (5) can be rewritten as follows:

$$I_t = I_{ph} - I_{sd1}\left[\exp\left(\frac{q(V_t + R_s \cdot I_t)}{n_1 \cdot k \cdot T}\right) - 1\right] - I_{sd2}\left[\exp\left(\frac{q(V_t + R_s \cdot I_t)}{n_2 \cdot k \cdot T}\right) - 1\right] \ldots - I_{sd3}\left[\exp\left(\frac{q(V_t + R_s \cdot I_t)}{n_3 \cdot k \cdot T}\right) - 1\right] - \frac{V_t + R_s \cdot I_t}{R_{sh}} \tag{6}$$

From Eq. (6) the value of I_{sd3} is affected by the same parameters that I_{sd1} and I_{sd2} in DD. The TD model has nine parameters that control the relationship between current and voltage in the SC. These parameters are R_s, R_{sh}, I_{ph}, I_{sd1}, I_{sd2}, I_{sd3}, n_1, n_2 and n_3.

Table 1 describes the ranges where are defined the parameters for the three models and they are used in this article for the experiments. In Table 1 the values of I_{sd1}, I_{sd2} and I_{sd3} in the TD and DD are the same that $I_{ph}(A)$ in the SD model. It is important to mention that the ranges in Table 1 were introduced in 1986 [7] and now they are widely used in the related literature. Some examples of their use for parameter estimation of solar cells are the implementation of the biogeography-based optimization algorithm with mutation strategies [39] and the application of the Lambert W-function [40]. Moreover, the limits defined in Table 1 are not selected randomly they should have physical meaning to have the desired performance in the SC [41]. In this sense, there exist some rules according to how to select the maximum and minimum values for the limits maintain a physical meaning [41]. On the other hand, it is important to mention that the ranges of Table 1 have tolerances that permit to create a feasible search space.

2.4. Solar cells parameter estimation as an optimization problem

From the mathematical models of SD, DD and TD is possible to consider each of them as a global optimization problem. First is necessary to define an objective function that is used to verify if a set of parameters is good or not according to a dataset. In other words, a good solution produces an accurate approximation between the I-V measurements from the physical SC and the values from the mathematical model. For the SD the error function is then defined as [42]:

$$f_{SD}(V_t, I_t, \mathbf{x}) = I_t - x_3 + x_4\left[\exp\left(\frac{q(V_t + x_1 \cdot I_t)}{x_5 \cdot k \cdot T}\right) - 1\right] + \frac{V_t + x_1 \cdot I_t}{x_2} \tag{7}$$

For the DD a similar equation is defined:

Table 1
The range of the parameters of SC.

Parameter	Upper value	Lower value
R_s (Ω)	0.5	0
R_{sh} (Ω)	100	0
I_{ph} (A)	1	0
I_{sd} (μA)	1	0
n	2	1

$$f_{\mathrm{DD}}(V_t, I_t, \mathbf{x}) = I_t - x_3 + x_4\left[\exp\left(\frac{q(V_t + x_1 \cdot I_t)}{x_6 \cdot k \cdot T}\right) - 1\right] \ldots + x_5\left[\exp\left(\frac{q(V_t + x_1 \cdot I_t)}{x_7 \cdot k \cdot T}\right) - 1\right] + \frac{V_t + x_1 \cdot I_t}{x_2} \tag{8}$$

Finally, for the TD the error equation is:

$$f_{\mathrm{TD}}(V_t, I_t, \mathbf{x}) = I_t - x_3 + x_4\left[\exp\left(\frac{q(V_t + x_1 \cdot I_t)}{x_6 \cdot k \cdot T}\right) - 1\right] + x_5\left[\exp\left(\frac{q(V_t + x_1 \cdot I_t)}{x_7 \cdot k \cdot T}\right) - 1\right] \ldots + x_8\left[\exp\left(\frac{q(V_t + x_1 \cdot I_t)}{x_9 \cdot k \cdot T}\right) - 1\right] + \frac{V_t + x_1 \cdot I_t}{x_2} \tag{9}$$

From Eqs. (7)–(9) the values of $V_t$and $I_t$are measurements from the real SC. In Eq. (7), $\mathbf{x} = [R_s,\ R_{sh},\ I_{ph},\ I_{sd},\ n]$ is solution vector, while, for the DD model $\mathbf{x} = [R_s,\ R_{sh},\ I_{ph},\ I_{sd1},\ I_{sd2},\ n_1,\ n_2]$ and for the TD model $\mathbf{x} = [R_s,\ R_{sh},\ I_{ph},\ I_{sd1},\ I_{sd2},\ I_{sd3},\ n_1,\ n_2,\ n_3]$. The functions f_{SD}, f_{DD} and f_{TD} measure the similarity of the output of each circuit with the desired value regarding current. The optimization problem then is defined as finding the configuration parameters that reduce the error that exist between the I_t estimated by diode models and the I_t desired. Here is necessary to use a set of N_E samples, then the objective function is the RMSE that is defined as:

$$RMSE(\mathbf{x}) = \sqrt{\frac{1}{N}\sum_{c=1}^{N_E}\left(f_M^c(V_t^c, I_t^c, \mathbf{x})\right)^2}, \tag{10}$$

In Eq. (10), M helps to choose the diode model that is evaluated. A dataset must be used it can be taken from the manufacturer documentation or experimentally created using different measurements. Considering the above the values of the dataset contains imprecise values no matter if they are selected directly from the manufacturers. Such affectations can be considered as noise that affects not only the performance of the SC (or PV panel) but also generates multimodal search spaces where the parameters to search are defined. These facts considerably influence the performance of the search strategies [43].

3. Whale optimization algorithm and opposition-based learning

This section aims to introduce the theory related to the standard Whale Optimization Algorithm (WOA) and the concepts of the Opposition-Based Learning (OBL).

3.1. Whale optimization algorithm

The Whale Optimization Algorithm (WOA) emulates the hunting behavior of humpback whales [27]. To search for the prey location and attack, the whales use two mechanisms. In the first one, the preys are encircled and the second consist in creates bubble nets. From an optimization point of view; the exploration of the search space is performed when the whales looking for a prey and the exploitation occurs during the attack behavior.

In WOA the bubble-nets are simulated using a spiral movement. This process mimics the helix-shaped movement from real humpback whales. In other words, a whale $x(t)$ has a position that can be updated moving it in a spiral around the prey x_{best}. This procedure is mathematically defined as:

$$x(t+1) = D \odot e^{bl} \odot \cos(2\pi l) + x_{best}(t) \tag{11}$$

where $D = |x(t) - x_{best}(t)|$ is the distance between $x(t)$ and $x_{best}(t)$ at the iteration t, $l \in [-1, 1]$ is a random number and b is a constant variable used to define the logarithmic spiral shape.

The whales can update their positions, using the encircling behavior [27], based on $x_{best}(t)$ as follows:

$$\begin{aligned} D &= |C \odot x_{best}(t) - x(t)| \\ x(t+1) &= x_{best}(t) - A \odot D \end{aligned} \tag{12}$$

The C and A are coefficient vectors, and are they are defined as:

$$\begin{aligned} C &= 2r \\ A &= 2a \odot r - a \end{aligned} \tag{13}$$

where r is a random vector and a is linearly decreased from 2 to 0 along the iterations (t), the value of a is thencomputed as in Eq. (14).

$$a = a - t\frac{a}{t_{\max}} \tag{14}$$

Accordingo the standard WOA [27] the whales can simultaneously swim around their prey along a spiral-shaped path and through a shrinking circle. This behavior is defined in Eq. (15).

$$x(t+1) = \begin{cases} x_{best}(t) - A \odot D & \text{if} \quad r_1 < 0.5 \\ D \odot e^{bl} \odot \cos(2\pi l) + x_{best}(t) & \text{otherwise} \end{cases} \tag{15}$$

where $r_1 \in [0, 1]$ is the probability of select the method of swim around the prey (the spiral model or shrinking encircling mechanism). However, the humpback whales may be searching for prey in a random form, and its position is updated based on a randomly selected whale $x_{rand}(t)$ as follows:

$$\begin{aligned} D &= |C \odot x_{rand}(t) - x(t)| \\ x(t+1) &= x_{rand}(t) - A \odot D \end{aligned} \tag{16}$$

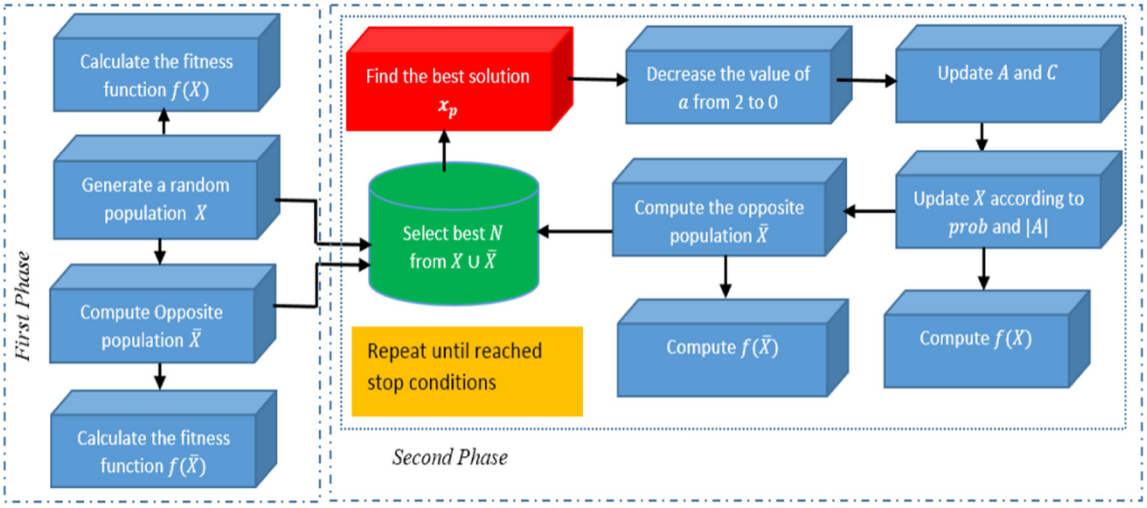

Fig. 4. The proposed method OBWOA.

Table 2
Set of benchmark optimization functions.

ID	Equation	Lower	Upper	Num. of dimensions	Type
F1	$f(x) = \sum_{i=1}^{n} x_i^2$	−100	100	10	Unimodal
F2	$f(x) = \sum_{i=1}^{n} \lvert x_i\rvert + \prod_{i=1}^{n} \lvert x_i\rvert$	−10	10	10	Unimodal
F3	$f(x) = \sum_{i=1}^{n} \left(\sum_{j-1}^{i} x_i \right)^2$	−100	100	10	Unimodal
F4	$f(x) = \max_i\{\lvert x_i\rvert, 1 \leqslant i \leqslant n\}$	−100	100	10	Unimodal
F5	$f(x) = \sum_{i=1}^{n-1} [100(x_{i+1} - x_i^2)^2 + (x_i - 1)^2]$	−30	30	10	Unimodal
F6	$f(x) = \sum_{i=1}^{n} ([x_i + 0.5])^2$	−100	100	10	Unimodal
F7	$f(x) = \sum_{i=1}^{n} i \cdot x_i^4 + random[0, 1]$	−1.28	1.28	10	Unimodal
F8	$f(x) = \sum_{i=1}^{n} -x_i \sin(\sqrt{x_i})$	−500	500	10	Multimodal
F9	$f(x) = \sum_{i=1}^{n} [x_i^2 - 10\cos(2\pi x_i) + 10]$	−5.12	5.12	10	Multimodal
F10	$f(x) = -20\exp\left(-0.2\sqrt{\frac{1}{n}\sum_{i=1}^{n} x_i^2}\right) - \exp\left(\frac{1}{n}\sum_{i=1}^{n}\cos(2\pi x_i)\right) + 20 + e$	−32	32	10	Multimodal
F11	$f(x) = \frac{1}{4000}\sum_{i=1}^{n} x_i^2 - \prod_{i=1}^{n}\cos\left(\frac{x_i}{\sqrt{i}}\right) + 1$	−600	600	10	Multimodal
F12	$f(x) = \frac{\pi}{n}\left\{10\sin^2(\pi y_1) + \sum_{i=1}^{n-1}(y_i - 1)^2[1 + 10\sin^2(\pi y_{i+1})] + (y_n - 1)^2\right\}$ $\sum_{i=1}^{n} u(x_i, 10, 100, 4)$ $u(x_i, a, k, m) = \begin{cases} k(x_i - a)^m, & x_i > a \\ 0, & -a \leqslant x_i \leqslant a \\ k(-x_i - a)^m, & x_i < -a \end{cases}$	−50	50	10	Multimodal
F13	$f(x) = 0.1\left\{\sin^2(3\pi x_i) + \sum_{i=1}^{n}(x_i - 1)^2[1 + \sin^2(3\pi x_i + 1)] + (x_n - 1)^2[1 + \sin^2(2\pi x_n)]\right\} + \sum_{i=1}^{n} u(x_i, 5, 100, 4)$	−50	50	10	Multimodal
F14	$f(x) = \left(\frac{1}{500} + \sum_{j=1}^{25}\frac{1}{j + \sum_{i=1}^{2}(x_i - a_{ij})^6}\right)^{-1}$	−65.536	65.536	2	Multimodal
F15	$f(x) = \left(\sum_{i=1}^{11}\left[a_i - \frac{x_1(b_i^2 + b_i x_2)}{b_i^2 + b_i x_3 + x_4}\right]^2\right)$	−5	5	4	Multimodal
F16	$f(x) = \left(4x_1^2 - 2.1x_1^4 + \frac{1}{3}x_1^6 + x_1x_2 - x_2^2 + 4x_2^4\right)$	−5	5	2	Multimodal
F17	$f(x) = \left(x_2 - \frac{5.1}{4\pi^2}x_1^2 + \frac{5}{\pi}x_1 - 6\right)^2 + 10\left(1 - \frac{1}{8\pi}\right)\cos x_1 + 10$	−5	5	2	Multimodal
F18	$f(x) = [1 + (x_1 + x_2 + 1)^2(19 - 14x_1 + 3x_1^2 - 14x_2 + 6x_1x_2 + 3x_2^2)] \times [30 + (2x_1 - 3x_2) \times (18 - 32x_1 + 12x_1^2 + 48x_2 - 36x_1x_2 + 26x_2^2)]$	−2	2	2	Multimodal
F19	$f(x) = -\sum_{i=1}^{4} c_i \exp\left(-\sum_{j=1}^{3} a_{ij}(x_j - p_{ij})^2\right)$	1	3	3	Multimodal
F20	$f(x) = -\sum_{i=1}^{4} c_i \exp\left(-\sum_{j=1}^{6} a_{ij}(x_j - p_{ij})^2\right)$	0	1	6	Multimodal
F21	$f(x) = -\sum_{i=1}^{5}[(X - a_i)(X - a_i)^T + c_i]^{-1}$	0	10	4	Multimodal
F22	$f(x) = -\sum_{i=1}^{7}[(X - a_i)(X - a_i)^T + c_i]^{-1}$	0	10	4	Multimodal
F23	$f(x) = -\sum_{i=1}^{10}[(X - a_i)(X - a_i)^T + c_i]^{-1}$	0	10	4	Multimodal

3.2. Opposition-based learning

This section presents the theory of the Opposition-Based Learning (OBL), this mechanism has been proposed to improve the exploration of Metaheuristic (MH) algorithms and ECA in optimization problems. Considering that in MH and ECA the first step is the random initialization of a population of a candidate solution, the information that each solution contains is crucial for a proper optimization. In the iterative process, the population is updated, and the and knowledge that stored in each element is used to obtain the new positions in the search space. In most of the cases, if this knowledge is not good or does not exist, they are used operators that generate random movements in the search spaces. Such situation can affect the convergence of the optimal global solution. In this context, the OBL is used to solve this drawback. It searches in the opposite direction, to the current solutio at the same time. Therefore, the exploitation of the search space increases and there exist more probabilities to find the globa optimal solution, this effect is reflected in the convergence of the optimization process.

Table 3
The comparison results between WOA and OBWOA.

Functions	Fitness Function		STD		Time		SR		Wilcoxon test	
	WOA	OBWOA	WOA	OBWOA	WOA	OBWOA	WOA	OBWOA	p	h
F1	2.1E−145	**0**	1.2E−144	**0**	**1003.177**	1013.047	100	100	1.2118e−12	1
F2	4.6E−99	**4.9E−301**	2.49E−98	**0**	1384.624	**1360.91**	100	100	2.3657e−12	1
F3	829614.8	**148413.1**	162,605	**108924.6**	**1189.252**	1299.154	0	0	1.9568e−10	1
F4	77.18557	**6.42E−51**	22.30	**2.99E−50**	**1042.52**	1057.235	0	100	3.0199e−11	1
F5	97.6875	**27.3243**	0.3914	**0.071362**	1378.60	**1201.75**	0	0	9.7917E−5	1
F6	1.74772	**0.003715**	0.6309	**0.00853**	979.778	**969.983**	0	3.3333	3.0199e−11	1
F7	**0.002707**	0.017502	**0.0033**	0.013734	**974.495**	990.601	0	16.666	9.8329E−8	1
F8	**−35795.1**	−41873.6	5230.99	**110.7154**	**963.647**	972.345	100	100	6.6955e−11	1
F9	**0**	**0**	**0**	**0**	965.526	**962.217**	100	100	NaN	0
F10	4.2E−15	**8.88E−16**	2.27E−15	**0**	968.402	**966.216**	100	100	3.0610E−9	1
F11	0.004124	**0**	0.0225	**0**	**971.654**	977.401	96.666	100	0.3337	0
F12	0.015771	**0.000235**	0.0063	**0.000228**	1350.802	**1337.615**	0	0	3.0199e−11	1
F13	1.563883	**0.004184**	0.6444	**0.003512**	**1352.934**	1345.346	0	0	3.0199e−11	1
F14	**1.819601**	4.06555	**1.8905**	3.527381	**1018.232**	1012.361	0	0	3.1981E−7	1
F15	0.000721	**0.000463**	**0.0004**	0.0004	971.456	**919.7368**	100	100	4.0840E−5	1
F16	**−1.03163**	−1.03151	**9.6E−11**	0.000455	951.561	**949.150**	100	100	1.2118e−12	1
F17	**0.397888**	**0.397924**	**1.15E−6**	0.000121	**1280.09**	1296.341	0	0	6.5250E−8	1
F18	3.000018	4.839737	**2.26E−5**	6.984354	961.110	**960.329**	0	0	2.2780E−5	1
F19	**−3.86274**	**−3.85917**	**8.8E−5**	0.047113	**954.476**	964.191	96.666	100	0.1120	0
F20	−3.32168	**−3.32015**	**0.0004**	0.11538	**1316.598**	1322.173	100	100	1.3111E−8	1
F21	−8.19969	**−10.1498**	2.6393	**0.01586**	**967.855**	985.844	63.333	100	1.0666E−7	1
F22	−9.16789	**−10.4013**	2.5362	**0.004579**	**965.569**	994.489	80	100	1.6062E−6	1
F23	−9.61889	**−10.5332**	2.0435	**0.009057**	5663.583	**5640.013**	83.333	100	1.1747	1

The best values obtained by WOA and OBWOA are in bold.

In OBL one of the central concepts is the opposite number $\bar{x}$ of real number x [31]. To compute the opposit position in one dimension it is used Eq. (17).

$$\bar{x} = u + l - x \tag{17}$$

where l and u represents the lowest and upper bounds of search domain, respectively. This defnition can be exdent to the multidimensional space [31]. Considering that $\mathbf{x} \in \mathbb{R}^n$ with $\mathbf{x} = [x_1, x_2, ..., x_n]$, where $x_i \in \mathbb{R}$. The defnition of the opposite point $\bar{\mathbf{x}} = [\bar{x}_1, \bar{x}_2, ..., \bar{x}_n]$ is given as:

$$\bar{x}_i = u_i + l_i - x_i, \quad i = 1, 2, ..., n \tag{18}$$

3.2.1. Opposition-based optimization

In the OBL method, the position **x** is replaced by its opposite $\bar{\mathbf{x}}$whenever the fitness function of $\bar{\mathbf{x}}$is better than the fitness function of **x,** otherwise **x** not saved. In this sense, the population is conformed only by the better values of the **x** or $\bar{\mathbf{x}}$(through comparing them) [11].

4. The proposed approach for solar cells design

The proposed OBWOA for solar cells design is described in this section. In the OBWOA the OBL is used to enhance the convergence of the standard WOA. Like other swarm algorithms, the traditional WOA can get stuck in local optimal point, and therefore the convergence becomes slow and time-consuming. This problem occurs because of some whales update their position based on the position of the best whale position (solution). However, the optimal solution might be in the opposite direction to the current solution. Considering such drawbacks, the proposed method avoids this problem by searching the global solution in both directions (forward and opposite).

The proposed approach consists of two phases: In the first step, the WOA is starting by generating a random solution then the OBL is used to improve the performance of the solutions by computing their opposite positions. In the second phase, the positions of the whales are updated based on the traditional strategy used in WOA. Then the OBL is also used to determine if the fitness function value of opposite solution is better than the updated solution or not. The two phases of the proposed method are explained in more details in the following subsections.

4.1. First phase

The proposed approach begins by creating a random population $X$with Nsolution (where the position $x_i = [x_{i1}, x_{i1}, ..., x_{in}]$, $i = 1, 2, ..., N$. Then the opposite positions are obtained by the OBL and they are used to construct the opposite population $\bar{\mathbf{x}}$. After that the best Npositions (solutions) are selected from $\mathbf{x} \cup \bar{\mathbf{x}}$.

The steps of this phase are as follows:

(1) Generate a population x of N solutions.
(2) Compute $\bar{\mathbf{x}}$ using Eq. (18).
(3) Select from $\mathbf{x} \cup \bar{\mathbf{x}}$ the best N solutions to produce a new population.

4.2. Second phase

In this stage, the positions of whales are updated by using the steps of the traditional WOA then the OBL approach is used again to generate the opposite positions $\bar{x}_i$, $i = 1, ..., N$. Afther that the OBWOA choose the best N psoitions from the union of the current population and its opposite population ($X \cup \bar{X}$) according to the fitness function values. The previous steps are performed again until the stop criteria is reached, the proposed OBWOA method is given in Fig. 4.

5. Experimental results

In order to evaluate the performance of the proposed method, a set of experimental series is performed. In which in the experimental series 1, a set of benchmark functions are used to assess the quality of the proposed method to find the optimal solution. Meanwhile, the experimental series 2 aims to test the performance of the proposed method to determine the optimal value of the parameters of single, double, and three diode models of solar cells. In addition, the experimental series 3 aims to estimation the Parameter of Photovoltaic panels. The last experimental series studies the influence of different irradiance levels on the proposed method.

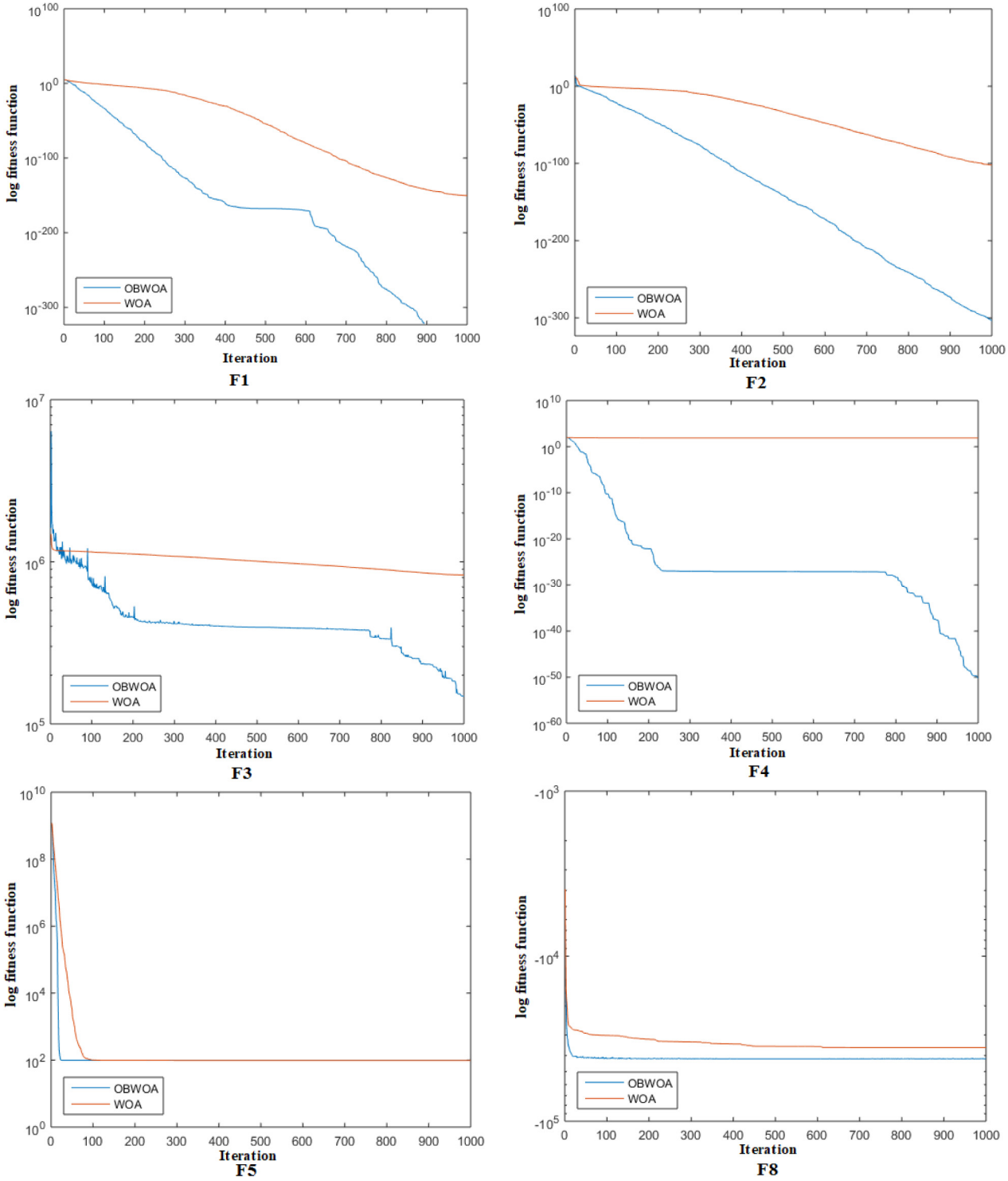

Fig. 5. The convergence curves for WOA and the proposed OBWOA along each test function.

5.1. Experimental series 1: test functions

In the experiments performed in this section, a set of benchmark functions is used to evaluate the accuracy of the proposed approach. It contains 23 functions distributed between multimodal (F8 to F23) and unimodal (F1 to F7). The definition and description these functions are given in Table 2 [44].

5.1.1. Parameters of the compared algorithms

For the WOA and the OBWOA maximum number of iterations is set as t_{max} = 1000 and the value of the parameter a is configured as a = 2. The experiments results are performed using "Windows 7 (64 bit)" that runs on "CPU Core2 Duo with 4 GB ram"; and "Matlab 2014b" software is used.

5.1.2. Measures of performance

In order to assess the performance of the compared algorithms according to the fitness function, they are used the following measures [45]:

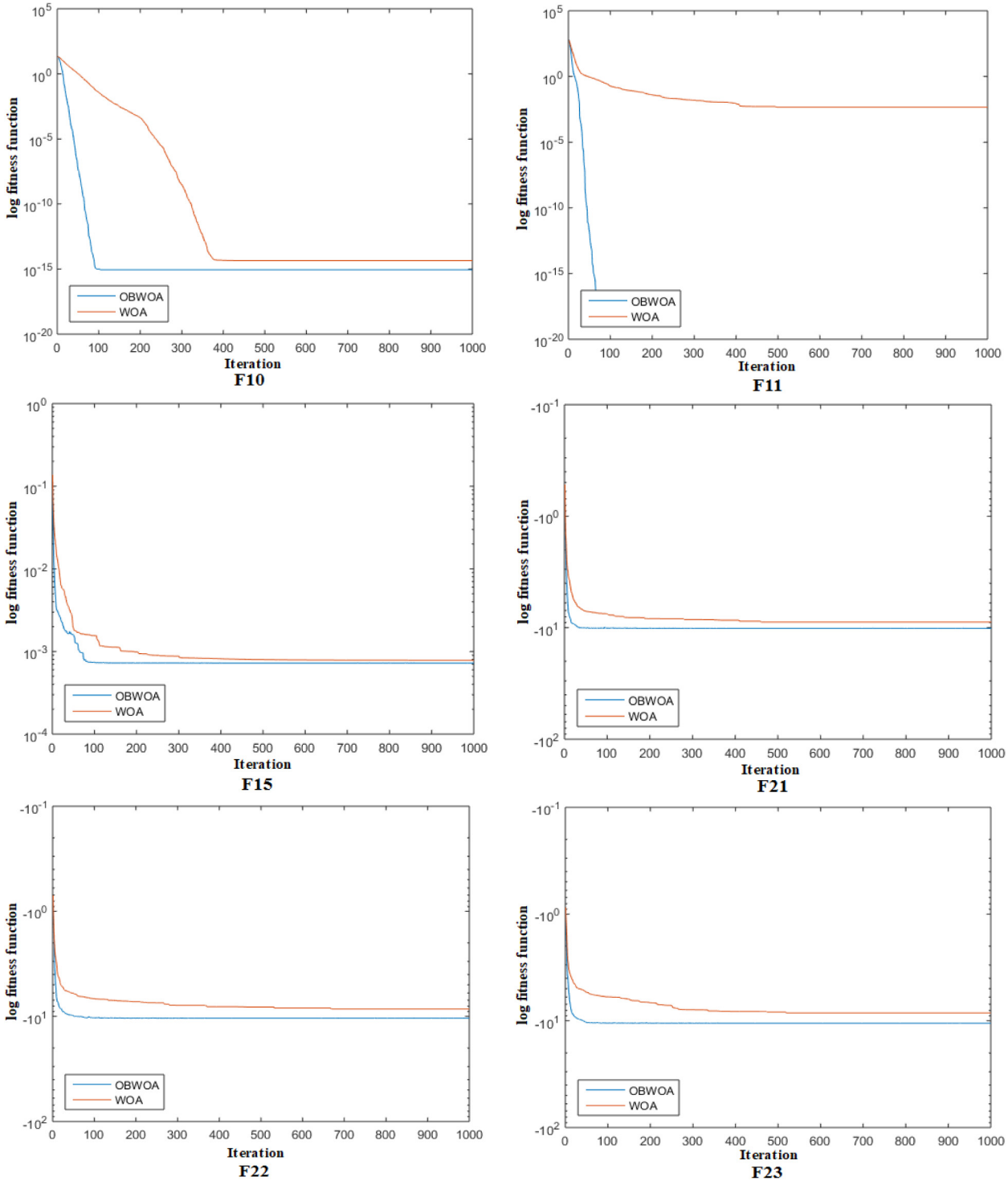

Fig. 5. (*continued*)

- *Mean* of fitness values that defined as:

$$Mean = \frac{1}{N_r}\sum_{i=1}^{N_r} F_i \tag{19}$$

- Standard Deviation (*STD*):

$$STD = \sqrt{\frac{1}{N_r - 1}\sum_{i=1}^{N_r} (F_i - Mean)^2} \tag{20}$$

- Success Rate (*SR*):

$$SR = \frac{NVTR}{N_r} \tag{21}$$

where N_r and *NVTR* represent the total number of runs and the total numbers that the algorithm reached to Value-To-Reach (VTR).

5.1.3. Comparison with WOA

In this section, the performance of the standard WOA is compared with the proposed OBWOA regarding fitness function value, STD, time complexity, and SR measures. The results of these comparisons are shown in Table 3 and Fig. 5. Based on the fitness function value the

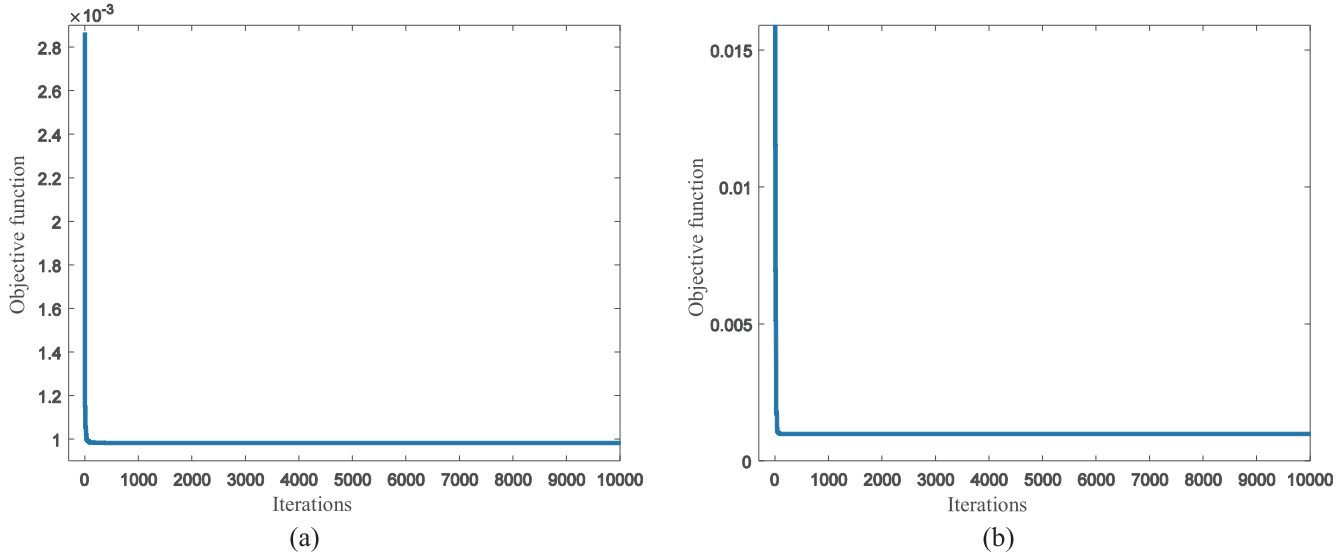

Fig. 6. The fitness function value with the number of iterations for (a) double diode model and (b) single diode model.

Table 4
The the real solar cells Dataset [48].

Data	V_{tm}(V) Measured	$I_{tm}(A)$ Measured	Data	V_{tm}(V) Measured	$I_{tm}(A)$ Measured
1	−0.2057	0.7640	14	0.4137	0.7280
2	−0.1291	0.7620	15	0.4373	0.7065
3	−0.0588	0.7605	16	0.4590	0.6755
4	0.0057	0.7605	17	0.4784	0.6320
5	0.0646	0.7600	18	0.4960	0.5730
6	0.1185	0.7590	19	0.5119	0.4990
7	0.1678	0.7570	20	0.5265	0.4130
8	0.2132	0.7570	21	0.5398	0.3165
9	0.2545	0.7555	22	0.5521	0.2120
10	0.2924	0.7540	23	0.5633	0.1035
11	0.3269	0.7505	24	0.5736	−0.0100
12	0.3585	0.7465	25	0.5833	−0.1230
13	0.3873	0.7385	26	0.5900	−0.2100

Table 5
The set of performance measures.

Name of Measure	Formula	Name of Measure	Formula
Relative Error R_{err}	$\frac{I_{tm}-I_{te}}{I_{te}} \times 100$	Normalized RMSE (NRMSE)	$\frac{RMSE}{\max(I_{te})-\min(I_{te})}$
Normalized Relative Error (NR_{err})	$\frac{R_{error}}{\max(I_{te})-\min(I_{te})}$	Mean Bias Error (MBE)	$\sum_{i=1}^{N_E} \frac{I_{tm}-I_{te}}{N_E}$
Mean Absolute Error (MAE)	$\sum_{i=1}^{N_E} \frac{\lvert I_t-I_{te}\rvert}{N_E}$	Normalize MBE (NMBE)	$\frac{MBE}{\max(I_{te})-\min(I_{te})}$
Normalized MAE (NMAE)	$\sum_{i=1}^{N_E} \frac{\lvert I_{tm}-I_{te}\rvert / I_t}{N_E}$	N_E: is the number of experimental dataN_E = 26. $\min(I_{te})$: is minimum values ofI_{te} $\max(I_{te})$: is maximum values ofI_{te}	

OBWOA is better than WOA in F1-F6, F10-F13, F15 and F20-F23. However, the traditional WOA obtains the best values in the functions (F7, F8, F14, F16 and F18). However, for Functions F9, F17 and F19, the two algorithms give the same results nearly. Also, based on the standard deviation, the proposed OBWOA is stable in most optimization functions except F7 and F14-F20 the WOA is the best. In term of time, in general, the two algorithms need the same time to reach the optimal value. However, WOA is fast in 12 functions and OBWOA is faster in 11 functions, but this difference is minimal between them.

Moreover, the reliability of the two algorithms is measured using the Success Rate (SR) as in Table 3. Based on these results it can be observed that the average of SR for the proposed OBWOA is ~9% higher than WOA (61.7391 versus 53.04339). Also, the two algorithms fail to find the solution for the functions F3, F5, F12-F14, F17, and F18.

In addition, Fig. 6 shows the convergence curve of the proposed OBWOA and the WOA algorithms. From this figure, it can be seen that the proposed OBWOA algorithm can converge faster than the WOA over all the tested functions, except F4. However, for F3, the OBWOA after less than 50 iterations becomes faster than WOA and this indicates the ability of OBL to improve the performance of the WOA algorithm.

In addition, the nonparametric Wilcoxon rank sum test is used to decide if there a significant difference between the WOA and OBWOA or not [46]. Where it depends on two hypotheses, the null and the alternative. Where the null hypothesis assumes that there not exists a significant difference between the OBWOA (that represents the control group) and WOA confidence interval 95% (i.e., significance level 5%).

The statistical results of Wilcoxon rank sum test are given in the last column in Table 3; in which from this table it can be seen the significant difference between OBWOA algorithm and the traditional WOA in all functions except F9, F11, and F19.

5.2. Experiment series 2: parameter estimation of solar cells for a standard data set

The performance of the OBWOA for the identification solar cell parameters is evaluated based on a set of experimental I–V data [23]. The outline of this section is then defined as follows: the description of the dataset, the definition performance metrics and the results of OBWOA for Single and Double and Three Diode model.

First, it is necessary to define the optimization problem. The parameters of each equivalent circuit (DD, SD, and TD) should be adapted as vectors that are considered as positions of whales. The number of parameters of the diode models defines the dimensionality of the optimization space. The limits that generate the search space is presented in Eq. (22).

Table 6
Terminal (V_t−I_t) measurements and the value of $R_{err}$and NR_{err}%for the SD and DD models.

Data	$I_{tm}(A)$ Measured	SD Model			DD Model		
		$I_{te}(A)$	R_{err}	NR_{err}% Normalized	$I_{te}(A)$	R_{err}	NR_{err}% Normalized
1	0.7640	0.7641	−0.0001	37.2740	0.7640	0.0000	39.1382
2	0.7620	0.7627	−0.0007	23.2850	0.7626	−0.0006	24.8540
3	0.7605	0.7614	−0.0009	18.5815	0.7613	−0.0008	19.8312
4	0.7605	0.7602	0.0003	47.6379	0.7602	0.0004	48.3955
5	0.7600	0.7591	0.0009	62.1028	0.7591	0.0009	62.4836
6	0.7590	0.7580	0.0010	62.3786	0.7581	0.0009	62.4934
7	0.7570	0.7571	−0.0001	36.9291	0.7572	−0.0001	36.9579
8	0.7570	0.7561	0.0009	59.9209	0.7562	0.0008	59.6033
9	0.7555	0.7551	0.0004	49.1090	0.7552	0.0004	48.6870
10	0.7540	0.7537	0.0003	47.2338	0.7537	0.0003	46.7091
11	0.7505	0.7514	−0.0009	17.5153	0.7514	−0.0009	17.1339
12	0.7465	0.7474	−0.0009	18.4407	0.7473	−0.0009	18.1278
13	0.7385	0.7401	−0.0016	0.0000	0.7400	−0.0016	0.0000
14	0.7280	0.7274	0.0006	54.2113	0.7273	0.0006	54.2196
15	0.7065	0.7070	−0.0005	27.8785	0.7069	−0.0005	28.4502
16	0.6755	0.6753	0.0002	44.7223	0.6752	0.0002	45.5952
17	0.6320	0.6308	0.0013	69.5066	0.6308	0.0013	70.5058
18	0.5730	0.5719	0.0011	65.3652	0.5720	0.0011	66.4584
19	0.4990	0.4996	−0.0006	24.6317	0.4997	−0.0006	25.8178
20	0.4130	0.4136	−0.0006	23.5105	0.4137	−0.0006	24.3611
21	0.3165	0.3175	−0.0010	14.6464	0.3175	−0.0010	15.1375
22	0.2120	0.2122	−0.0002	35.2765	0.2121	−0.0002	35.2708
23	0.1035	0.1023	0.0012	69.2550	0.1022	0.0012	68.8513
24	−0.0100	−0.0087	−0.0013	8.0300	−0.0088	−0.0013	8.1604
25	−0.1230	−0.1255	0.0025	100	−0.1255	0.0025	100
26	−0.2100	−0.2085	−0.0015	2.4942	−0.2084	−0.0015	3.7971

Table 7
The values of different performance measures for SD and DD models.

Model	Mean RMSE	Std (RMSE)	NRMSE	MAE	NMAE	NMBE
SD	9.8603	1.0196E−8	0.62593	8.28598	−0.00532	11.8677
DD	9.8294	1.1278E−7	0.6257	8.19258	−0.0049	11.7231

$$\text{minimize: } RMSE(\mathbf{X}),\quad \mathbf{X}=[\mathbf{x}_{w1},\mathbf{x}_{w2},...,\mathbf{x}_{wN}],\quad \mathbf{x}_{wi}=[x_{i,1},x_{i,2},...x_{i,d}]\quad d\in[5,7,9],$$

$$\begin{array}{lccc} & d=5\ (\text{SD}) & d=7(\text{DD}) & d=9(TD) \\ \text{subject to:} & 0\leqslant x_{i,1}(R_s)\leqslant 0.5 & 0\leqslant x_{i,1}(R_s)\leqslant 0.5 & 0\leqslant x_{i,1}(R_s)\leqslant 0.5 \\ & 0\leqslant x_{i,2}(R_{sh})\leqslant 100 & 0\leqslant x_{i,2}(R_{sh})\leqslant 100 & 0\leqslant x_{i,2}(R_{sh})\leqslant 100 \\ & 0\leqslant x_{i,3}(I_{ph})\leqslant 1 & 0\leqslant x_{i,3}(I_{ph})\leqslant 1 & 0\leqslant x_{i,3}(I_{ph})\leqslant 1 \\ & 0\leqslant x_{i,4}(I_{sd})\leqslant 1 & 0\leqslant x_{i,4}(I_{sd1})\leqslant 1 & 0\leqslant x_{i,4}(I_{sd1})\leqslant 1 \\ & 1\leqslant x_{i,5}(n)\leqslant 2 & 0\leqslant x_{i,5}(I_{sd2})\leqslant 1 & 0\leqslant x_{i,5}(I_{sd2})\leqslant 1 \\ & & 1\leqslant x_{i,6}(n_1)\leqslant 2 & 0\leqslant x_{i,6}(I_{sd3})\leqslant 1 \\ & & 1\leqslant x_{i,7}(n_2)\leqslant 2 & 1\leqslant x_{i,7}(n_1)\leqslant 2 \\ & & & 1\leqslant x_{i,8}(n_2)\leqslant 2 \\ & & & 1\leqslant x_{i,9}(n_3)\leqslant 2 \end{array} \tag{22}$$

5.2.1. Data set description

A comercial silicon solar cell of 57 mm of diameter is used for this experiment. It operates under standard test conditions defined as 1 sun) 1000 W/m^2) at T = 33 °C. Moreover, four additional temperatures have been included (T = 25 °C, T = 50 °C, T = 75 °C and T = 100 °C) to verify the efficiency of the proposed approach. Following [47], the search domain for unknown parameters of SC models is given in Table 1 and Eq. (13). The data given in Table 4, contains 26 samples and it has been used in many related works [47]. Also, Table 4 shows the original data, voltage (V_{tm}) and current (I_{tm}) extracted from the real solar cells. The parameters of the algorithm are set as N = 150, N = 150, $itern$ = 10,000.

5.2.2. Performance measurement for the parameter estimation of solar cells

To evaluate the quality of the results obtained by the proposed algorithm for the problem of SC parameter estimation, it is used a set of different metrics that are presented in Table 5.

5.2.3. Case of study 1: single diode and double diode models

The results of the OBWOA to identify the parameters of SC using SD

Table 8
The results of the OBWOA for the SD model.

Parameter	OBWOA	HS	GGHS	IGHS	LMSA	ABSO	CWOA	OFPANM
I_{ph} (A)	0.76077	0.7607	0.7609	0.7608	0.7608	0.7608	0.76077	0.7607755
I_{sd} (μA)	0. 3232	0.3050	0.3262	0.3435	0.3185	0.3062	0.3239	0.3230208
n	1.5208	1.4754	1.4822	1.4874	1.4798	1.4758	1.4812	0.0363771
R_s (Ω)	0. 0363	0.0366	0.0363	0.0361	0.0364	0.0366	0.03636	53.7185203
R_{sh} (Ω)	53.6836	53.5946	53.0647	53.2845	53.3264	52.2903	53.7987	1.4811836
RMSE	9.8602	9.9510	9.9097	9.9306	9.8640	9.9124	9.8602	9.8602
	BMO	Rcr − IJADE	STLBO	GOTLBO	ABC	CSO	CIABC	
I_{ph} (A)	0.76077	0.76086	0.76078	0.76078	0.7608	0.7608	0.760776	
I_{sd} (μA)	0.32479	0.32302	0.32302	0.33155	0.3251	0.3230	0.32302	
n	1.48173	1.48118	1.48114	1.48382	1.4817	1.4812	1.48102	
R_s (Ω)	0.03636	0.03638	0.03638	0.03627	0.0364	0.0364	0.036377	
R_{sh} (Ω)	53.8716	53.71853	53.7187	54.11543	53.6433	53.7185	53.71867	
RMSE	9.8608	9.8602	9.8602	9.87442	9.862	9.8602	9.8602	

Table 9
The results of the OBWOA the DD model.

Parameters	OBWOA	IGHS	ABSO	CSO	BMO	Rcr − IJADE	STLBO	GOTLBO	ABC	CWOA	CIABC	OFPANM
I_{ph} (A)	0.76076	0.76079	0.76078	0.76078	0.76078	0.760781	0.760780	0.760752	0.7608	0.76077	0.760781	0.760781
I_{sd1} (μA)	0.2299	0.9731	0.26713	0.22732	0.21110	0.225974	0.225660	0.800195	0.0407	0.24150	0.227828	0.749347
I_{sd2} (μA)	0.61956	0.16791	0.38191	0.72785	0.87688	0.03674	0.036740	0.036783	0.2874	0.60000	0.647650	0.2259743
n_1	1.49154	1.92126	1.46512	1.45151	1.44533	1.451017	1.450850	1.448974	1.4495	1.45651	1.451623	2.000000
n_2	2	1.42814	1.98152	1.99769	1.99997	2	2	1.999973	1.4885	1.9899	1.988343	1.451016
R_s (Ω)	0.03671	0.0369	0.03657	0.036737	0.03682	0.749347	0.752170	0.220462	0.0364	0.03666	0.036728	0.036740
R_{sh} (Ω)	55.399	56.8368	54.6219	55.3813	55.8081	55.48544	55.49200	56.075304	53.7804	55.2016	55.37826	55.48544
RMSE	9. 8251	9.8635	9.8344	9.8252	9.8262	9.8248	9.8248	9.83177	9.861	9. 8272	9.8262	9.8248

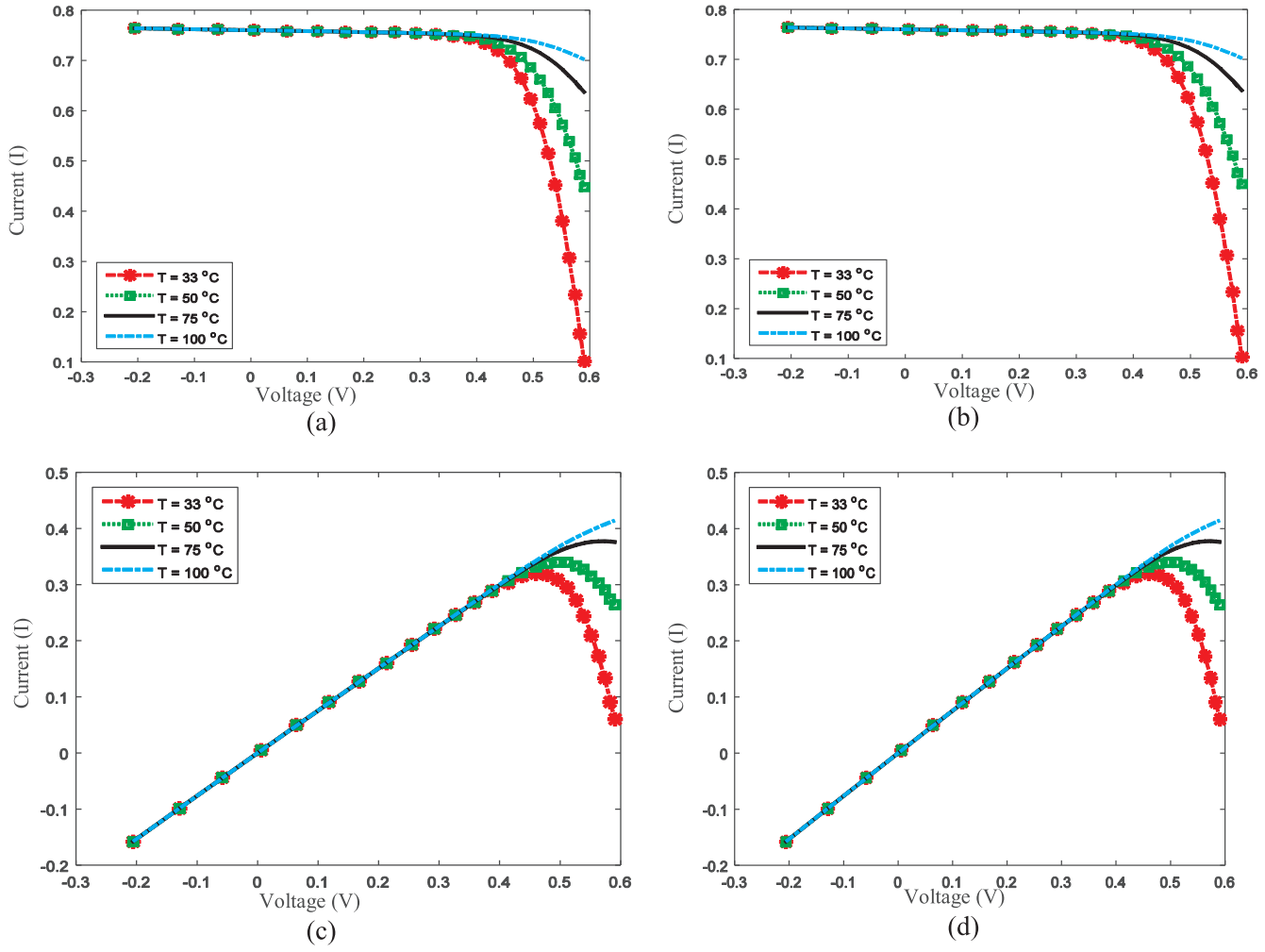

Fig. 7. Measured voltage vs. OBWOA calculated current for (a) SD model, (b) DD model. Measured voltage vs. OBWOA-power for (c) SD model, (d) DD model, all at T = 33°, T = 50°, T = 75° and T = 100°.

Table 10
Parameter estimation of three diode model using ABC, OBWOA, and STBLO.

Parameters	ABC	OBWOA	STBLO
I_{ph} (A)	0.7607	0.76077	0.7608
I_{sd1} (μA)	0.2000	0.2353	0.2349
I_{sd2} (μA)	0.50	0.2213	0.2297
I_{sd2} (μA)	0.2100	0.4573	0.4443
n_1	1.4414	1.4543	1.4541
n_2	1.9	2	2
n_3	2	2	2
R_s (Ω)	0.03687	0.03668	0.0367
R_{sh} (Ω)	55.8344	55.4448	55.2641
RMSE	9.8466	9.8249	9.8253

and DD models are compared with other related algorithms. For example, the Generalized Oppositional Teaching Learning Based Optimization (GOTLBO) [49], that also employs the theory of OBL. The Repaired Crossover Rate Adaptive DE (Rcr-IJADE) [50], this method includes different modifications like a new crossover operator that permit to obtain more accurate results in the estimation of parameter of SC. The Innovative Global Harmony Search (IGHS) uses an elite of solutions to generate new harmonies [21], this method has been applied for SC parameter identification [21]. Other methods also used for comparisions are the Levenberg–Marquardt algorithm combined with simulated annealing (LMSA) [51], the Artificial Bee Swarm Optimization (ABSO) [52] that is based on the behavior of honey bees. The Grouping-Based Global Harmony Search (GGHS) [21], where the

Table 11
The average results of the ABC, OBWOA and STBLO algorithms.

Model	RMSE	Std (RMSE)	NRMSE	MAE	NMAE	NMBE
OBWOA	9.850	2.4739E−5	0.6259	8.18732	−0.00501	11.8879
ABC	9.8466	1.2790	0.6257	8.14407	−0.0045	11.6517
STBLO	9.8253	2.5204E−5	0.6263	8.1864	−0.0054	12.1228

solutions are divided in different groups to generate more accurate solutions. The Cat Swarm Optimization (CSO) [19] inspired by the behaviour of cats, the STLBO [22] that is inspired in the teaching process. The Artificial Bee Colony (ABC) [47] that mimics the bees mechanis for searching food sources, the Bird Matting Optimizer (BMO) [53] that imitates the behavior of bird species metaphorically to breed broods with superior genes. The Chaotic Whale Optimization Algorithm [23], the Flower Pollination Algorithm simultaneously combined with the OBL and the NM simplex method (OFPANM) [54] and finally the Chaotic Improved Artificial Bee Colony (CIABC) [24]. These algorithms are selected for the comparsion, because of they established their performance in literature.

The results of OBWOA to estimate the current I_e for both models (SD and DD) are given in Table 6, and this results are evaluated using R_{err} and NR_{err}. From this table it can be seen that the values of R_{err} are found in the interval [−1.60E−3, 2.50E−3] for both models, which indicates that the SD model estimated by OBWOA is success to describe the actual behavior of SC. Furthermore, the values of each performance measure is given Table 7 which point to the high accuracy and stability of the OBWOA approach for estimate the parameters of two models.

Moreover, Fig. 6 shows the convergence accuracy of the proposed approach during iteration process for SD and DD models, respectively. From this figure, it is observed that after ~500 iterations the relative stability of the objective function occurs.

In addition the results of comparison the OBWOA with other algorithms for SD model and DD model are given in Tables 8 and 9, respectively. From Table 8, the SD model case the RMSE of the proposed method is better than the other algorithms except for Rcr-IJADE, CWOA, CIABC, STLBO and CSO algorithms which have the same RMSE value.

In the same context, the results of the OBWOA for DD model are listed in Table 9. This table provide evidence that the proposed approach better than IGHS, ABSO, GOTLBO and ABC algorithms. Meanwhile, the Rcr-IJADE and STLBO are better than the proposed method based on RMSE value, also, the CIABC is better than CWOA, CSO and BMO, however, accuracy of these four algorithms are less than the OBWOA (in general, the difference between the Rcr-IJADE, CSO, BMO, OBWOA, and STLBO is minimal).

The current vs. voltage and power vs. voltage are computed at a different degree of temperatures such as 33, 50, 75 and 100 °C according to the estimated parameters by OBWOA. The results are given in Fig. 7 for the SD and DD models, from this figure it can be observed that the two SC models (SD and DD) have high ability to represent the real photovoltaic cell characteristics. Since the proposed OBWOA can (nearly) estimate the optimal parameter values, the obtained approximation for I_t is more accurate. However, the temperatures affect the current values in the OBWOA and also the power values, but even with this disturbance, the OBWOA method can find the best solution. From Fig. 7 is important to mention that the plots are obtained using the experimental voltage and the computed current presented Table 4. The experimental data has been extensively employed in the related literature [15]. It contains negative voltage values, for that reason, there are obtained negative power values [23]. The same situation occurs for the plot of current vs. voltage. However, the aim of parameter estimation is reducing the MSRE that exist between the values contained in the data set and the values computed by the models. OBWOA can fit the experimental values in all cases no matter how they are obtained.

5.2.4. Case of study 2: three diode model

In order to investigate the performance of the proposed approach to identify the parameters of three diode model, it has been compared with the ABC [55] and STBLO algorithms [22]. The results of are listed in Tables 10 and 11. From such tables, it can be observed that the RMSE of the proposed method is better than the other two algorithms, whereas, the STBLO is better than ABC.

Moreover, according to the NRMSE, MAE, NMAE and NMBE values, it can be concluded that the OBWOA and ABC have better results than the STBLO algorithm. However, the ABC is a little better than OBWOA except regarding NMBE in which the OBWOA has a better performance. Additionally, the value of Std for the proposed OBWOA indicates the high stability and reliability it to achieve the high-quality RMSE value.

In the same context, to add further evidence about the quality of the proposed OBWOA to estimate the parameters of three diode model. The estimated current obtained by the ABC, STBLO and OBWOA are plotted at T = 51 °C in Fig. 8. It is observed from this figure that the OBWOA and ABC have the better estimation than STBLO algorithm.

5.2.5. Experiment series 3: parameter estimation of photovoltaic panels

In this experiment, another real dataset is used to evaluate the performance of the proposed OBWOA. The information is extracted from the Monocrystalline PV panel [48]. The model of the commercial solar panel is STM6-40/36. It is manufactured by the company Schutten Solar abd contains a 36 Monocrystalline cells with a size 38 mm × 128 mm connected in series.

To correctly compute the I of the Monocrystalline PV panel, Eq. (2)

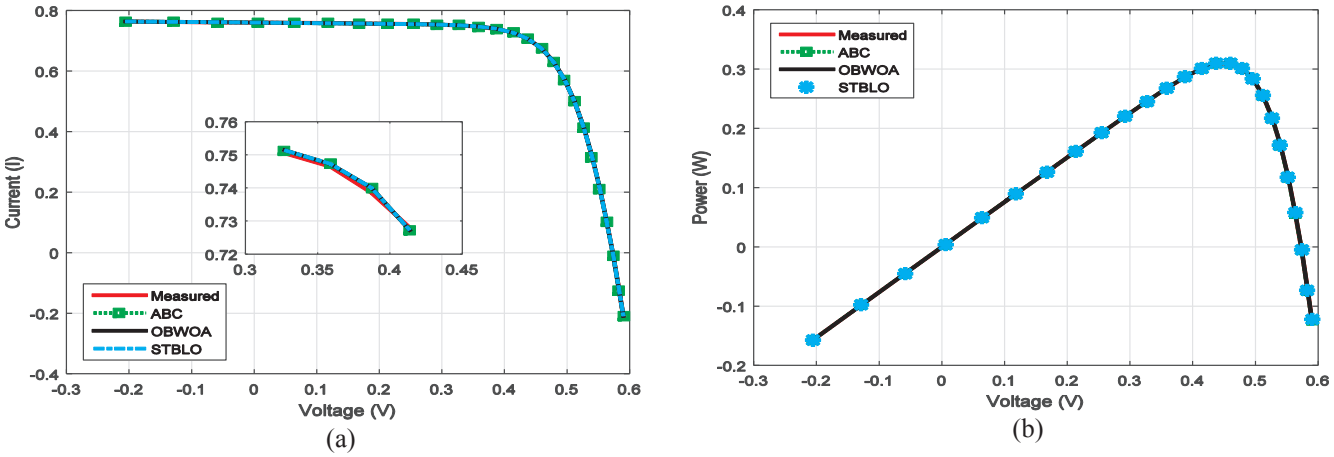

Fig. 8. The estimation of the proposed method for (a) current and (b) power.

Table 12
The estimated current and its Error (E) using data from solar panel based on Monocrystalline.

Data	Measured		Ref. [48]		BMO		ABC		CWOA		CIABC		STBLO		OBWOA	
	V	I (A)	I (A)	E×10^{-4}	I (A)	E×10^{-4}	I (A)	E×10^{-4}	I (A)	E×10^{-4}	I (A)	E×10^{-4}	I (A)	E×10^{-4}	I (A)	E ×10^{-4}
1	0.118	1.663	1.6627	1.80	1.663	−3.31	1.664	−4.50	1.6637	4.25	1.664	−3.18	1.6638	−4.86	1.6634	−2.95
2	2.237	1.661	1.659	12.1	1.6596	8.09	1.660	6.79	1.6598	6.75	1.660	7.51	1.6598	6.85	1.6605	2.42
3	5.434	1.653	1.6531	−60.5	1.6537	−4.47	1.654	−5.91	1.6540	6.37	1.654	−6.10	1.6538	−5.22	1.6539	−5.86
4	7.26	1.65	1.6497	1.82	1.6502	−1.47	1.650	−2.96	1.6506	3.64	1.651	−3.63	1.6503	−1.93	1.6504	−2.73
5	9.68	1.645	1.6445	3.04	1.6449	25.5	1.645	−1.20	1.6453	2.08	1.645	−2.39	1.6449	0.207	1.6452	−1.28
6	11.59	1.64	1.6383	10.4	1.6387	7.62	1.639	6.44	1.6390	5.61	1.639	5.13	1.6386	7.96	1.6396	2.13
7	12.6	1.636	1.633	18.4	1.6333	16.5	1.633	15.7	1.6335	15.0	1.634	14.5	1.6332	17.1	1.6335	14.7
8	13.37	1.629	1.6267	14.1	1.6269	12.3	1.627	11.9	1.6271	11.5	1.627	11.0	1.6268	13.2	1.6279	6.70
9	14.09	1.619	1.6171	11.7	1.6181	5.00	1.618	5.15	1.6181	5.03	1.618	4.60	1.6180	6.13	1.6174	9.89
10	14.88	1.597	1.603	−37.4	1.6032	−38.8	1.603	−37.8	1.6030	37.5	1.603	−37.8	1.6029	−37.3	1.6028	−36.2
11	15.59	1.581	1.582	−6.32	1.5819	−6.14	1.582	−4.26	1.5815	3.60	1.582	−3.76	1.5816	−4.28	1.582	−6.32
12	16.4	1.542	1.5432	−7.78	1.5429	−6.43	1.543	−3.41	1.5423	2.48	1.542	−2.45	1.5426	−4.17	1.5437	−11.0
13	16.71	1.524	1.5225	9.85	1.5219	13.6	1.521	17.1	1.5212	18.0	1.521	18.1	1.5215	16.0	1.5219	13.8
14	16.98	1.5	1.5006	−4.00	1.4999	0.253	1.499	3.93	1.4992	4.80	1.499	4.94	1.4995	2.69	1.4993	4.27
15	17.13	1.485	1.4867	−11.4	1.4860	−7.05	1.485	−3.27	1.4853	2.47	1.485	−2.30	1.4856	−4.61	1.4853	−2.68
16	17.32	1.465	1.4674	−16.4	1.4664	−9.61	1.466	−5.78	1.4657	5.10	1.466	−4.91	1.4660	−7.20	1.4658	−5.54
17	17.91	1.388	1.3897	−12.2	1.3880	−0.598	1.388	2.56	1.3876	2.52	1.388	2.69	1.3878	1.27	1.3877	2.02
18	19.08	1.118	1.1208	−25.0	1.1169	9.33	1.118	−0.5	1.1181	1.78	1.118	−2.00	1.1175	3.75	1.1188	−7.95

Table 13
The Estimated Parameters and their accuracy for the dataset from solar panel based on Monocrystalline.

Parameter	Ref. [48]	BMO	STBLO	CWOA	ABC	OBWOA	CIABC
R_s(m)	4.879	5.00	5.00	5.00	4.99	4.4	4.40
R_{sh}	15.419	14.9371	15.40	15.4	15.206	15.5299	15.617
I_{ph}	1.4142	1.6646	1.7000	1.7	1.6644	1.6642	1.6760
I_{sd}(μ)	1.6635	1.4311	1.4127	1.6338	1.50	1.65025	1.6642
n	1.4986	1.4994	1.5	1.5	1.4866	1.51424	1.4976
MAE	0.001722	0.001308	0.00127	0.00122003	0.001229	0.001199	0.001206
RMSE	0.002181	0.001900	0.001900	0.0018	0.0018379	0.001753	0.001819
NMAE	0.00153	0.000838	0.000804	0.00076963	0.0007728	0.0007692	0.00076
NRMSE	0.004026	0.003476	0.003478	0.00329967	0.00336812	0.0032181	0.0033372

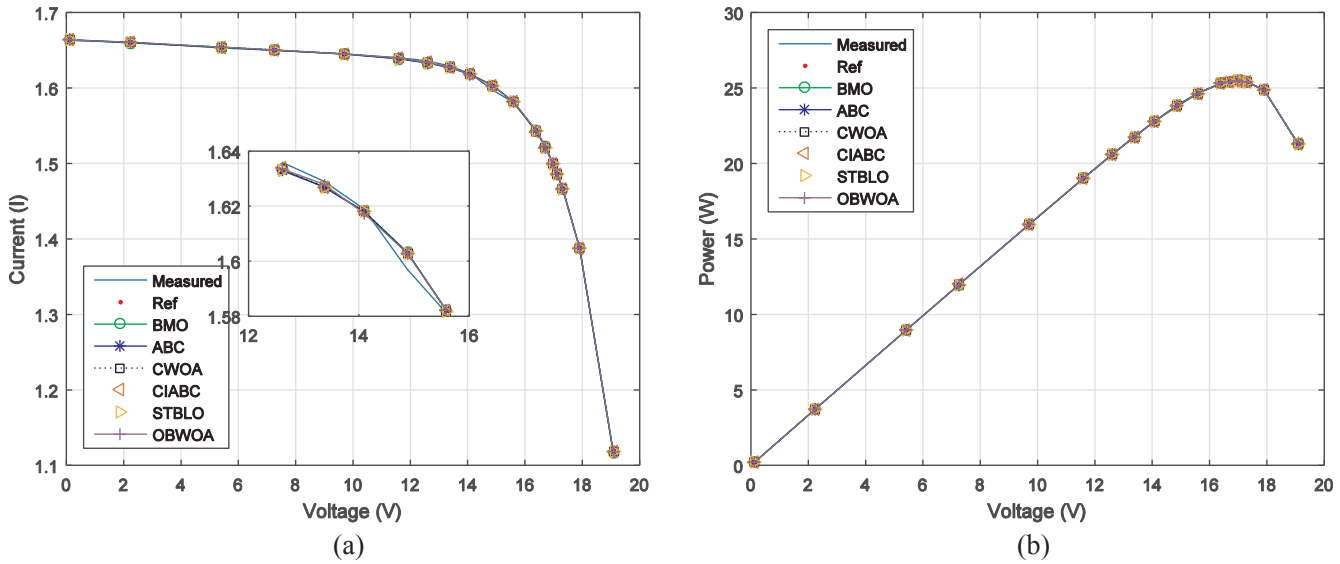

Fig. 9. The results of each algorithm to estimate (a) current and (b) power using solar panel based on monocrystalline.

has been rewritten as the follows:

$$I_{te} = I_{ph} - I_{sd}\left[\exp\left(\frac{(V_t + M\cdot R_s\cdot I_{te})}{n\cdot k\cdot T\cdot M/q}\right) - 1\right] - \frac{V_t + M\cdot R_s\cdot I_{te}}{M\cdot R_{sh}} \quad (23)$$

The *I-V* data is presented in Table 13; it has been recorded from this panel at Temperature T = 51 °C. The current of the SC (I_{SC} = 1.663 A) has been measured at short-circuit, the voltage value is V_{OC} = 21.02 V and it is obtained when the cells are open-circuited. The output current of the panels is I_M = 1.50 A and terminal voltage is V_M = 16.98 V, they are measured operating at the maximum power point.

5.2.5.1. Case of study 1: single diode and double diode models. The performance of the proposed OBWOA is evaluated based only on the SD model, and it is compared with STBLO, ABC, CWOA, CIABC, BMO

Table 14
The Estimated Parameters using the proposed method and their accuracy for Multi-crystalline S75 at different irradiance levels.

	SD					DD					TD				
	1000 W/m^2	800 W/m^2	600 W/m^2	400 W/m^2	200 W/m^2	1000 W/m^2	800 W/m^2	600 W/m^2	400 W/m^2	200 W/m^2	1000 W/m^2	800 W/m^2	600 W/m^2	400 W/m^2	200 W/m^2
I_{ph}	4.6897	3.8048	2.7438	1.9013	0.9801	4.6809	3.7694	2.8801	1.9231	0.8876	4.234	3.9861	3.1801	2.9910	0.9476***
I_{sd1}	0.0351	0.0019	0.0004	0.0066	0.0402	0.1201	0.6601	0.00008	0.6203	0.0054	0.3201	0.7619	0.0009	0.5638	0. 9028
I_{sd2}	–	–	–	–	–	0.0239	0.0034	0.0008	0.0066	0.0498	0.3972	0.0049	0.0005	0.0078	0.282
I_{sd3}	–	–	–	–	–	–	–	–	–	0.8341	0.9188	0.8640	0.86675	0.5169	0.9931
R_s	0.2603	0.3689	0.4114	0.2660	0.2090	0.2594	0.3520	0.3922	0.2660	0.2621	0.6012	0.578	0.4271	0.6012	0.2086
R_{sh}	373.1888	373.7701	318.4056	349.1298	415.3398	373.5981	425.9310	298.1452	350.9872	411.7831	379.0911	439.143	352.982	379.651	444.446
n_1	1.2301	1.0698	0.9981	1.1309	1.2499	3.5701	3.9401	0.9991	4.000	2.7102	3.5701	3.9401	0.9991	1.451	1.1721
n_2	–	–	–	–	–	1.2301	1.1109	1.0350	1.1499	1.2421	2.2130	2.199	2.309	2.099	2.1
n_3	–	–	–	–	–	–	–	–	–	–	3.78	3.93	4.00	4.000	3.91
RMSE	0.0247	0.0209	0.0205	0.0091	0.0017	0.0243	0.0199	0.0204	0.0090	0.00148	0.0231	0.0195	0.0203	0.0089	0.00145

and the results presented in reference [48] (in the remainder text it is called *Ref*).

The comparison results of the OBWOA and the other algorithms based on a set of measures are given in Tables 12 and 13 , as well as; the current is computed based on the extracted parameters using each algorithm. From these results, it can be seen that the OBWOA has better va lues according to RMSE, MAE, NMAE, and NRMSE measures except NMAE the CIABC is the better. Moreover, the CWOA, ABC and the CIABC have the better results than the other algorithms. However, the CIABC has the best results, followed by the CWOA then the ABC that allocate the third rank. Also, all these algorithms give results better than that obtained by *Ref*.

Fig. 9 shows the power vs. voltage and current vs. voltage that computed at the degree of temperature equal to 51 °C according to the extracted parameters by each algorithm. From this figure, it can be seen that, in general, all the algorithms fail to reach the measured data as shown in Fig. 9(a). However, the OBWOA is closed to measured data better than the other algorithms.

5.2.6. Experiment series 4: the influence of different irradiance levels on the proposed method

In order to further evaluate the practicability of the proposed algorithm, in this section, it is used to extract the optimal parameters for the SC Multi-crystalline S75 [56]. The OBWAOA use the three diode models (SD, DD, and TD). The experimental data at different irradiance levels were extracted from the (I-V) curves given in the manufacturer's data sheets. Here a five irradiance levels are used including 1000 W/m^2, 800 W/m^2, 600 W/m^2, 400 W/m^2, and 200 W/m^2 at temperature 25 °C. However, in some cases the measurements not aviable. In such situations the search range of I_{ph} is determined based on the data sheet parameters of each module at STC: short circuit current $I_{SC_{STC}}$ and temperature coefficient for short circuit current α [38]. Where, the I_{SC} at non-standard conditions are computed as in the following equation:

$$I_{SC}(G, T) = I_{SC_{STC}} * \frac{G}{G_{SC}} + \alpha(T - T_{STC})$$

where T and G represent temperature and irradiance, respectively. Then, the search range for I_{ph}, I_{sd}, R_s, R_s and n is set as $[0, 2I_{SC}](A)$, $[0, 1](\mu A)$, $[0, 2](\Omega)$, $[0, 5000](\Omega)$ and $[0, 4]$, respectively.

The estimated parameters of the three diode models along the five irradiance levels are given in Table 14. Meanwhile, Fig. 10 depicted the experimental data and the estimated models. It can be seen from Fig. 10 that, the I-V curves of the estimated TD models is very close to the experimental data at all irradiance levels overall the irradiance levels (that used in this study). As well as, the accuracy of the proposed model at irradiance level 200 W/m^2 is better than at other irradiance levels. Morever, from Table 14, it can be observed that, the values of $R_s < 0.7$. In PV modules, usually the value of Rs is very low, meanwhile the value of R_{sh} is very high.

6. Conclusions

A new modified version of the Whale Optimization Algorithm (WOA) based on the opposition–based learning is proposed to extract the parameters of the photovoltaic cell. The OBL strategy is used to improve the convergence of the WOA at two steps: (1) at the initialization of the population and (2) when the population is updated. To evaluate the performance of the proposed OBWOA method, a set of experiment series are performed. In the first set, the proposed method is compared against the classical WOA using 23 benchmark functions that have different characteristics. According to the results provided in this experiment, it has been concluded that the OBWOA has better performance than the standard WOA in terms of all performance metrics. Meanwhile, the experiment series 2 aims to test the effect of the proposed OBWOA method to extract the parameters of PV cells using standard datasets. The results of OBWOA are compared with other

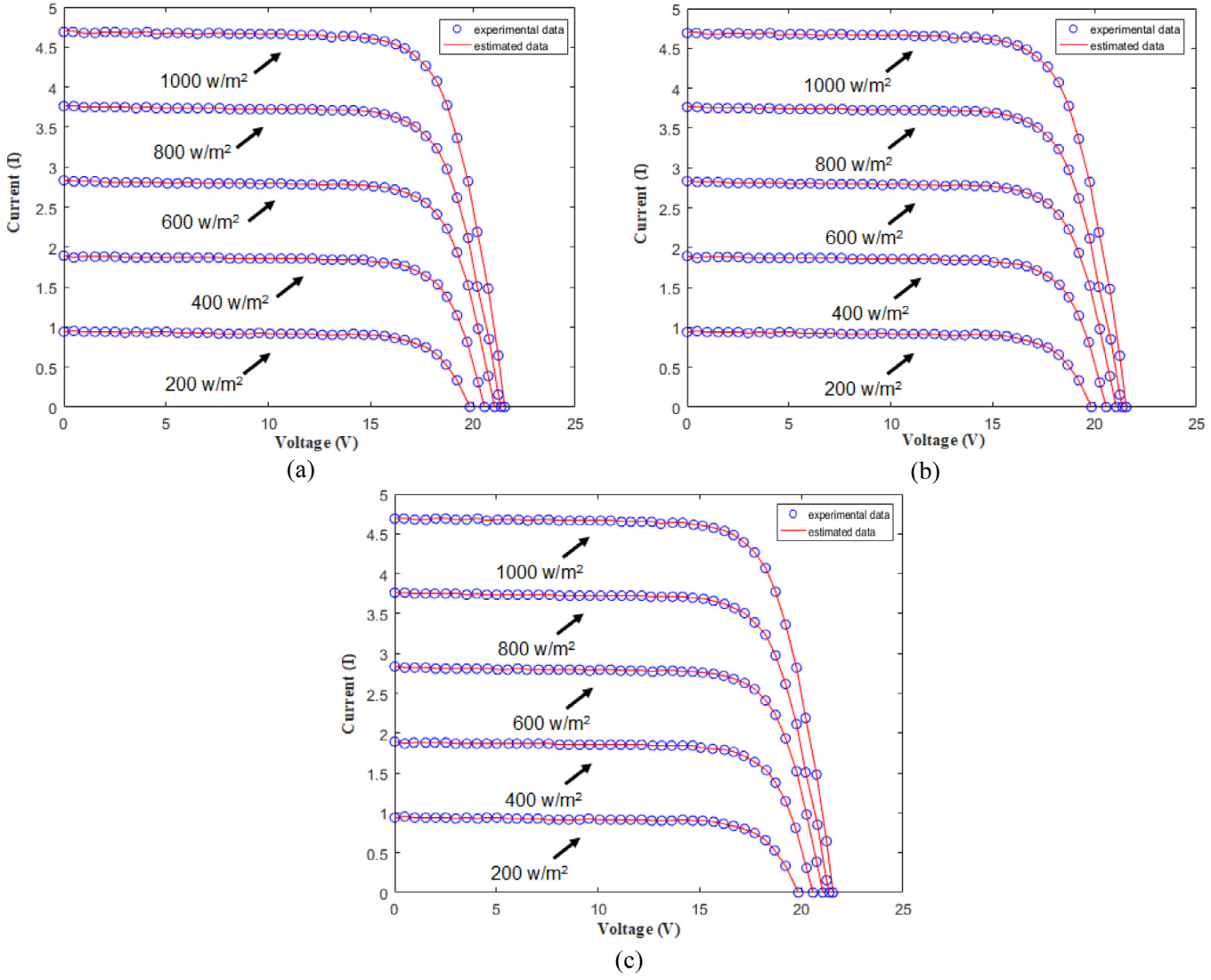

Fig. 10. Comparison between the estimated model and the experimental data of multi-crystalline S75 at different irradiance for (a) SD model, (b) DD model, (c) TD model.

similar algorithms different at three cases of study (Single Diode, Double Diode and Three Diode model). The results refer to the high performance of OBWOA regarding the metrics used to evaluate the quality of the estimated parameters. The Third experiments series provides another evidence about the quality of the OBWOA to estimate the parameters of Monocrystalline PV panels. The results of OBWOA are compared with different optimization algorithms, and it stills provide a high performance according to the single diode model. In addition, from the last experiments series, it can be concluded the proposed method gives accurate results at different irradiance levels using Multi-crystalline S75.

Considering the effectiveness of the OBWOA's results, in the future work it may be applied to different fields as medical image processing and data mining. Some problems from such fields where OBWA can be used are (1) Image segmentation, (2) Feature selection and (3) Engineering design. Also, the performance of OBWOA can be increased by combining it with other optimization algorithms to the exploitation of prominent regions of the search space.

References

[1] Arshad M. Chapter three – clean and sustainable energy technologies. Elsevier Inc.; 2017. https://doi.org/10.1016/B978-0-12-805423-9.00003-X.

[2] Sampaio PGV, González MOA. Photovoltaic solar energy: conceptual framework. Renew Sustain Energy Rev 2017;74:590–601. http://dx.doi.org/10.1016/j.rser.2017.02.081.

[3] REN 21. Renewables 2017: global status report; 2017. https://doi.org/10.1016/j.rser.2016.09.082.

[4] Ma T, Yang H, Lu L. Solar photovoltaic system modeling and performance prediction. Renew Sustain Energy Rev 2014;36:304–15. http://dx.doi.org/10.1016/j.rser.2014.04.057.

[5] Lo Brano V, Orioli A, Ciulla G, Di Gangi A. An improved five-parameter model for photovoltaic modules. Sol Energy Mater Sol Cells 2010;94:1358–70. http://dx.doi.org/10.1016/j.solmat.2010.04.003.

[6] Khanna V, Das BK, Bisht D, Vandana PK Singh. A three diode model for industrial solar cells and estimation of solar cell parameters using PSO algorithm. Renew Energy 2015;78:105–13. http://dx.doi.org/10.1016/j.renene.2014.12.072.

[7] Easwarakhanthan T, Bottin J, Bouhouch I, Boutrit C. Nonlinear minimization algorithm for determining the solar cell parameters with microcomputers. Int J Sol Energy 1986;4:1–12. http://dx.doi.org/10.1080/01425918608909835.

[8] Gao X, Cui Y, Hu J, Xu G, Yu Y. Lambert W-function based exact representation for double diode model of solar cells: comparison on fitness and parameter extraction. Energy Convers Manage 2016;127:443–60. http://dx.doi.org/10.1016/j.enconman.2016.09.005.

[9] Ortiz-Conde A, García Sánchez FJ, Muci J. New method to extract the model parameters of solar cells from the explicit analytic solutions of their illuminated I-V characteristics. Sol Energy Mater Sol Cells 2006;90:352–61. http://dx.doi.org/10.1016/j.solmat.2005.04.023.

[10] Chan DSH, Phillips JR, Phang JCH. A comparative study of extraction methods for solar cell model parameters. Solid State Electron 1986;29:329–37. http://dx.doi.org/10.1016/0038-1101(86)90212-1.

[11] Orioli A, Di Gangi A. A procedure to calculate the five-parameter model of crystalline silicon photovoltaic modules on the basis of the tabular performance data.

Appl Energy 2013;102:1160–77. http://dx.doi.org/10.1016/j.apenergy.2012.06.036.
[12] Appelbaum J, Peled A. Parameters extraction of solar cells - a comparative examination of three methods. Sol Energy Mater Sol Cells 2014;122:164–73. http://dx.doi.org/10.1016/j.solmat.2013.11.011.
[13] Li Y, Huang W, Huang H, Hewitt C, Chen Y, Fang G, et al. Evaluation of methods to extract parameters from current-voltage characteristics of solar cells. Sol Energy 2013;90:51–7. http://dx.doi.org/10.1016/j.solener.2012.12.005.
[14] Elbaset AA, Ali H, Abd-El Sattar M. Novel seven-parameter model for photovoltaic modules. Sol Energy Mater Sol Cells 2014;130:442–55. http://dx.doi.org/10.1016/j.solmat.2014.07.016.
[15] Alam DF, Yousri DA, Eteiba MB. Flower pollination algorithm based solar PV parameter estimation. Energy Convers Manage 2015;101:410–22. http://dx.doi.org/10.1016/j.enconman.2015.05.074.
[16] Jervase JA, Bourdoucen H, Al-Lawati A. Solar cell parameter extraction using genetic algorithms. Meas Sci Technol 2001;12:1922–5. http://dx.doi.org/10.1088/0957-0233/12/11/322.
[17] Ye M, Wang X, Xu Y. Parameter extraction of solar cells using particle swarm optimization. J Appl Phys 2009;105. http://dx.doi.org/10.1063/1.3122082.
[18] El-Naggar KM, AlRashidi MR, AlHajri MF, Al-Othman AK. Simulated annealing algorithm for photovoltaic parameters identification. Sol Energy 2012;86:266–74. http://dx.doi.org/10.1016/j.solener.2011.09.032.
[19] Guo L, Meng Z, Sun Y, Wang L. Parameter identification and sensitivity analysis of solar cell models with cat swarm optimization algorithm. Energy Convers Manage 2016;108:520–8. http://dx.doi.org/10.1016/j.enconman.2015.11.041.
[20] Rajasekar N, Krishna Kumar N, Venugopalan R. Bacterial foraging algorithm based solar PV parameter estimation. Sol Energy 2013;97:255–65. http://dx.doi.org/10.1016/j.solener.2013.08.019.
[21] Askarzadeh A, Rezazadeh A. Parameter identification for solar cell models using harmony search-based algorithms. Sol Energy 2012;86:3241–9. http://dx.doi.org/10.1016/j.solener.2012.08.018.
[22] Niu Q, Zhang H, Li K. An improved TLBO with elite strategy for parameters identification of PEM fuel cell and solar cell models. Int J Hydrogen Energy 2014;39:3837–54. http://dx.doi.org/10.1016/j.ijhydene.2013.12.110.
[23] Oliva D, El Aziz MA, Hassanien AE. Parameter estimation of photovoltaic cells using an improved chaotic whale optimization algorithm. Appl Energy 2017. http://dx.doi.org/10.1016/j.apenergy.2017.05.029.
[24] Oliva D, Ewees AA, El Aziz MA, Hassanien AE, Cisneros MP. A chaotic improved artificial bee colony for parameter estimation of photovoltaic cells. Energies 2017;10. http://dx.doi.org/10.3390/en10070865.
[25] Valdivia-González A, Zaldívar D, Cuevas E, Pérez-Cisneros M, Fausto F, González A. A chaos-embedded gravitational search algorithm for the identification of electrical parameters of photovoltaic cells. Energies 2017;10:1–25. http://dx.doi.org/10.3390/en10071052.
[26] Allam D, Yousri DA, Eteiba MB. Parameters extraction of the three diode model for the multi-crystalline solar cell/module using Moth-Flame Optimization Algorithm. Energy Convers Manage 2016;123:535–48. http://dx.doi.org/10.1016/j.enconman.2016.06.052.
[27] Mirjalili S, Lewis A. The whale optimization algorithm. Adv Eng Softw 2016;95:51–67. http://dx.doi.org/10.1016/j.advengsoft.2016.01.008.
[28] Mostafa A, Hassanien AE, Houseni M, Hefny H. Liver segmentation in MRI images based on whale optimization algorithm. Multimed Tools Appl 2017:1–24. http://dx.doi.org/10.1007/s11042-017-4638-5.
[29] Dinakara Prasasd Reddy P, Veera Reddy VC, Gowri Manohar T. Whale optimization algorithm for optimal sizing of renewable energy resources for loss reduction in distribution systems. J Electr Syst Inf Technol 2017:1–13. http://dx.doi.org/10.1016/j.jesit.2017.06.001.
[30] Ling Y, Zhou Y, Luo Q. Lévy flight trajectory-based whale optimization algorithm for global. Optimization 2017;5:1–19. http://dx.doi.org/10.1109/ACCESS.2017.2695498.
[31] Tizhoosh HR. Opposition-based learning: a new scheme for machine intelligence. Int Conf Comput Intell Model Control Autom Int Conf Intell Agents, Web Technol Internet Commer 2005;1:695–701. http://dx.doi.org/10.1109/CIMCA.2005.1631345.
[32] Cuevas E, Oliva D, Zaldivar D, Perez-Cisneros M, Pajares G. Opposition-based electromagnetism-like for global optimization. Int J Innov Comput Inf Control; 2012. < http://www.scopus.com/inward/record.url?eid=2-s2.0-84870288971&partnerID=MN8TOARS > .
[33] Ma X, Liu F, Qi Y, Gong M, Yin M, Li L, et al. MOEA/D with opposition-based learning for multiobjective optimization problem. Neurocomputing 2014;146:48–64. http://dx.doi.org/10.1016/j.neucom.2014.04.068.
[34] Ahandani MA, Alavi-Rad H. Opposition-based learning in shuffled frog leaping: an application for parameter identification. Inf Sci (Ny) 2015;291:19–42. http://dx.doi.org/10.1016/j.ins.2014.08.031.
[35] Bulbul SMA, Pradhan M, Roy PK, Pal T. Opposition-based krill herd algorithm applied to economic load dispatch problem. Ain Shams Eng J 2015. http://dx.doi.org/10.1016/j.asej.2016.02.003.
[36] Abd ElAziz M, Oliva D, Xiong S. An improved opposition-based sine cosine algorithm for global optimization. Expert Syst Appl 2017. http://dx.doi.org/10.1016/j.eswa.2017.07.043.
[37] Chegaar M, Ouennoughi Z, Guechi F, Langueur H. Determination of solar cells parameters under illuminated conditions. J Electron Dev 2003;2:17–21.
[38] Steingrube S, Breitenstein O, Ramspeck K, Glunz S, Schenk A, Altermatt PP. Explanation of commonly observed shunt currents in c-Si solar cells by means of recombination statistics beyond the Shockley-Read-Hall approximation. J Appl Phys 2011;110. http://dx.doi.org/10.1063/1.3607310.
[39] Niu Q, Zhang L, Li K. A biogeography-based optimization algorithm with mutation strategies for model parameter estimation of solar and fuel cells. Energy Convers Manage 2014;86:1173–85. http://dx.doi.org/10.1016/j.enconman.2014.06.026.
[40] Jain A, Kapoor A. Exact analytical solutions of the parameters of real solar cells using Lambert W-function. Sol Energy Mater Sol Cells 2004;81:269–77. http://dx.doi.org/10.1016/j.solmat.2003.11.018.
[41] Laudani A, Riganti Fulginei F, Salvini A. Identification of the one-diode model for photovoltaic modules from datasheet values. Sol Energy 2014;108:432–46. http://dx.doi.org/10.1016/j.solener.2014.07.024.
[42] Jordehi AR. Parameter estimation of solar photovoltaic (PV) cells: a review. Renew Sustain Energy Rev 2016;61:354–71. http://dx.doi.org/10.1016/j.rser.2016.03.049.
[43] Beyer H-G. Evolutionary algorithms in noisy environments: theoretical issues and guidelines for practice. Comput Methods Appl Mech Eng 2000;186:239–67. http://dx.doi.org/10.1016/S0045-7825(99)00386-2.
[44] Abd Elaziz M, Oliva D, Xiong S. An improved opposition-based sine cosine algorithm for global optimization. Expert Syst Appl 2017;90. http://dx.doi.org/10.1016/j.eswa.2017.07.043.
[45] Suganthan PN, Hansen N, Liang JJ, Deb K, Chen Y-P, Auger A, et al. Special session on constrained real-parameter optimization. KanGAL 2006;2005:251–6.
[46] Wilcoxon F. Individual comparisons by ranking methods. Biometr Bull 1945;1:80. 10.2307/3001968.
[47] Oliva D, Cuevas E, Pajares G. Parameter identification of solar cells using artificial bee colony optimization. Energy 2014;72:93–102. http://dx.doi.org/10.1016/j.energy.2014.05.011.
[48] Tong NT, Pora W. A parameter extraction technique exploiting intrinsic properties of solar cells. Appl Energy 2016;176:104–15. http://dx.doi.org/10.1016/j.apenergy.2016.05.064.
[49] Chen X, Yu K, Du W, Zhao W, Liu G. Parameters identification of solar cell models using generalized oppositional teaching learning based optimization. Energy 2016;99:170–80. http://dx.doi.org/10.1016/j.energy.2016.01.052.
[50] Gong Cai W, Zhihua. Parameter extraction of solar cell models using repaired adaptive differential evolution. Sol Energy 2013;94:209–20.
[51] Dkhichi F, Oukarfi B, Fakkar A, Belbounaguia N. Parameter identification of solar cell model using Levenberg-Marquardt algorithm combined with simulated annealing. Sol Energy 2014;110:781–8. http://dx.doi.org/10.1016/j.solener.2014.09.033.
[52] Askarzadeh A, Rezazadeh A. Artificial bee swarm optimization algorithm for parameters identification of solar cell models. Appl Energy 2013;102:943–9. http://dx.doi.org/10.1016/j.apenergy.2012.09.052.
[53] Askarzadeh A, Rezazadeh A. Extraction of maximum power point in solar cells using bird mating optimizer-based parameters identification approach. Sol Energy 2013;90:123–33. http://dx.doi.org/10.1016/j.solener.2013.01.010.
[54] Xu S, Wang Y. Parameter estimation of photovoltaic modules using a hybrid flower pollination algorithm. Energy Convers Manage 2017;144:53–68. http://dx.doi.org/10.1016/j.enconman.2017.04.042.
[55] Oliva D, Cuevas E, Pajares G. Parameter identification of solar cells using artificial bee colony optimization. Energy 2014. http://dx.doi.org/10.1016/j.energy.2014.05.011.
[56] Shell Solar. Product information sheet shell S25 typical I/V characteristics; 2003. p. 75–6.